A Novel Multi-objective Evolutionary Algorithm with Dynamic Decomposition Strategy

Songbai Liu[1,2], Qiuzhen Lin[1]*, Ka-Chun Wong[2], Lijia Ma[1], Carlos A. Coello Coello[3], Dunwei Gong[4]

[1]*College of Computer Science and Software Engineering, Shenzhen University, Shenzhen, PR. China*

[2] *Department of Computer Science, City University of Hong Kong, Hong Kong, PR. China*

[3] *CINVESTAV-IPN, Department of Computer Science, Mexico, D.F., 07360, Mexico*

[4] *School of Information and Control Engineering, China University of Mining and Technology, Xuzhou 221116, Jiangsu, PR. China*

Abstract:

In this paper, a novel multi-objective evolutionary algorithm (MOEA) is proposed with dynamic decomposition strategy, called MOEA/D-DDS. After the recombination, all the parents and offspring populations both with the size N are combined as a union population in environmental selection, which is then associated to the preset N weight vectors using the constrained decomposition approach. By counting the number of solutions that fall within the feasible region of each subproblem, the number of subproblems that are not associated to any solution can be calculated and recorded by $T_{\max}$, which somehow shows the distribution of union population and also indicates the number of weight vectors (i.e., subproblems) to be regenerated. Then, the subproblem associated with the largest number of solutions will be found and then further divided into two new subproblems using the proposed dynamic decomposition strategy. This process of dynamic decomposition will be run $T_{\max}$ times in order to have N subproblems associated with at least one solution. At last, a simple convergence indicator is used to select one solution showing the best convergence for each of these N subproblems. Twenty-six well-known test problems are employed to challenge the performance of MOEA/D-DDS and the experiments validate the superiority of MOEA/D-DDS over six recently proposed MOEAs.

Keywords: Dynamic decomposition; Evolutionary algorithm; Multi-objective optimization

1. Introduction

Some practical applications (e.g., biology inference [1], data mining [2], power engineering [3], and optical networks [4]) can be naturally formulated as the problems to simultaneously optimize multiple (often conflicting) objectives [5] [6]. Due to the difficulties of solving multi-objective optimization problems (MOPs), they have attracted a great deal of attentions. Without loss of generality, this paper considers MOPs without any constraint, as defined by

$$Minimize \quad F(x) = (f_1(x), f_2(x), ..., f_m(x)) \tag{1}$$

* Corresponding author
Email address: songbai209@qq.com (S.B. Liu), qiuzhlin@szu.edu.cn (Q.Z. Lin)
Phone: +86-75526001223, Fax: +86-75526534078 (Q.Z. Lin)

Subject to $x \in \Omega$

where $x = (x_1, \ldots, x_n)$ is a decision vector with n dimensions and $F : \Omega \rightarrow R^m$ defines m objective functions (Ω and R^m are respectively the decision and objective spaces). Since the objectives often contradict with each other, no single solution can optimize them simultaneously. Thus, a MOP in Eq. (1) aims to find a Pareto-optimal set (PS), which has equally better solutions when considering all the objectives. The mapping of PS in the objective space is termed Pareto-optimal front (PF) [7]. For the purpose of supporting decision-makings in MOPs, it is necessary to search an approximate subset of PF that is closest to the true PF and evenly distributed along the true PF. Owing to the population-based nature of evolutionary algorithms (EAs), multi-objective EAs (MOEAs) are very popular for solving MOPs [9] [10], as they can search multiple solutions in a single run [8]. Generally, there are two goals for MOEAs to get a set of solutions, i.e., they approximate to the true PF as closely as possible (known as convergence) and they are distributed as evenly as possible along the true PF (known as diversity) [19]. To reach the above goals, a large number of MOEAs [11]-[16] were presented in the last decades. According to their selection strategies, most MOEAs can be classified into three main categories, i.e., Pareto-based MOEAs [11]-[12], indicator-based MOEAs [13]-[14], and decomposition- based MOEAs [15]-[16]. Pareto-based MOEAs use Pareto optimality definitions to guarantee the convergence and then further maintain the diversity with other metrics (e.g., crowding distance [11] or niching method [12]). Indicator-based MOEAs adopt performance indicator (e.g., Hyper-volume [17]) to guide the population's evolution, trying to balance the convergence and the diversity. Decomposition-based MOEAs transform MOPs into a set of subproblems, which are then solved by evolutionary search on a collaborative manner. The optimization of each subproblem ensures the convergence, while the use of the weight vectors evenly distributed in the objective space guarantees the diversity. Due to the easy implementation and good quantization property of decomposition-based MOEAs, they are becoming the major methodologies for tackling MOPs [18].

In a state-of-the-art decomposition-based MOEA (MOEA/D [15]), each individual is associated to optimize one subproblem by using the information from its neighboring subproblems. Simulated binary crossover (SBX) and polynomial mutation are adopted as the recombination operators in this original version. Moreover, the solution replacement in MOEA/D mainly depends on the aggregated function values to update the original solutions, aiming to speed up the convergence. However, as pointed out in [20], this method may lead to three main defects for MOEA/D, i.e., duplicate solutions, preset targets to be updated, and thoughtless deletion of solutions. To conquer these limitations and enhance performance of MOEA/D in solving different types of MOPs, a number of studies have been conducted based on MOEA/D, including the improved decomposition methods [21]-[26], the computational resource allocation strategies [27]-[29], the modified reproduction operators [30]-[35], the enhanced mating selection method [36], and the modified solution replacement approaches [37]-[42]. Overall,

these MOEA/D variants maintain the population's diversity by using a set of uniform weight vectors to define their subproblems and then renew the solution associated to each subproblem using the aggregated function values. However, this kind of solution replacement neglects the population's distribution in the objective space, which may hamper the diversity when solving some MOPs with irregular and discontinuous PFs.

To alleviate the above problem, constrained decomposition strategies for MOEA/D were suggested in [43]-[46], by transforming MOPs into a set of constrained subproblems. Each subproblem will be assigned with a constrained subspace in the objective space, regarded as its feasible region. Solutions inside the feasible region are always better than the outside solutions, which can maintain the population's diversity quite well. However, due to the inconsistency of the used weight vectors and the true PFs, this kind of constrained decomposition approaches often leads to the disequilibrium of solutions that are associated to subproblems, i.e., a larger number of solutions may be located in the feasible region of one subproblem, while no solution can be found in some feasible regions. Such cases will lead to the fact that their performances are very sensitive to the shapes of unknown PFs [47]. Generally, it often requires a user to select a suitable aggregation function with a specific set of weight vectors, in order to get superior performance on one particular MOP, which may not always be an easy task for no-experience users [44].

To solve the above problem, some adaptive adjustment approaches on the used weight vectors are designed in [48]-[52] based on the decomposition methods without any constraint. Working on the same research direction to adjust the weight vectors, this paper proposes a novel MOEA with dynamic decomposition strategy (DDS), called MOEA/D-DDS, which tries to regenerate the weight vectors under the constrained decomposition approach. In our DDS, N parent solutions and their N offspring solutions at each generation are combined to a union population with $2N$ solutions, which are then associated to the preset N uniform weight vectors based on the constrained decomposition method. Then, the distribution of union population can be shown by counting the number of solutions that fall in the feasible region of each subproblem, i.e., n_i $(i = 1, 2, ..., N)$ is used to record the number of solutions in the feasible region of ith subproblem with the constraint $\sum_{i=1}^{N} n_i = 2N$. By this way, the number of subproblems that are not associated to any solution can be calculated and recorded by $T_{\max}$, which also indicates the number of new weight vectors (subproblems) that need to be re-produced for associating solutions. Thereafter, the subproblem associated with the largest number of solutions will be found, which is further decomposed into two new subproblems using the proposed clustering-based method. Please note that when there are more than one subproblem associated with the largest number of solutions, one of them can be selected randomly. This dynamic decomposition process will be run $T_{\max}$ times in order to have N subproblems associated with at least one solution. At last, a simple convergence indicator is used to select one solution from the feasible region of each of these N

subproblems, which can simultaneously guarantee the convergence and the diversity even when the initially used weight vectors and evolutionary population are not so matched. When compared to six competitive MOEAs (NSGA-III [55], MOEA/D-DE [30], MOEA/D-DRA [27], MOEA/D-STM [37], MOEA/D-IR [41], and MOEA/D-ACD [43]), the experiments justify the advantages of MOEA/D-DDS in solving most cases of twenty-six well-known test MOPs.

The remainder of this paper is organized as follows. Section 2 introduces three decomposition approaches in MOEA/D and the constrained decomposition strategy. Section 3 introduces the details of MOEA/D-DDS, while Section 4 gives the experimental results and the corresponding discussions of MOEA/D-DDS with other competitors. Finally, Section 5 presents our conclusions and future work.

2. A short review of related work

2.1 Three decomposition approaches in MOEA/D

The motivation of using the idea of decomposition for solving MOPs may retrospect to C-MOGA [53] and cMOEA [54], which combine the traditional mathematical tool (i.e., the decomposition approach) with the heuristic search methods. In the original MOEA/D framework [15], there are two essential components for decomposition, i.e., the used decomposition function and the associated weight vectors. With these two elements, MOEA/D decomposes Eq. (1) into N scalar optimization subproblems, where N is the population size and also the number of weight vectors. Thereafter, it simultaneously optimizes all the N subproblems on a collaborative manner. The optimal solutions for N subproblems will approximate the entire true PF of a MOP. To enhance the performance of optimizing the subproblems, MOEA/D uses the information from neighboring subproblems as defined according to the Euclidean distance of weight vectors (i.e., the T closest weight vectors are considered as the T neighbors of subproblems), which helps to design a restricted mating selection method and a solution replacement strategy.

When generating the set of weight vectors $(\lambda^1,\lambda^2,...,\lambda^N)$, they are uniformly sampled from the unit hyperplane in the objective space, which can be determined by the user with priority or preset on a systematic manner. Based on the division parameter H and the condition $C_{H+m-1}^{m-1}=N$, each element $\lambda_j^i \in \lambda^i$ is assigned a value from the set $\{0,1/H,2/H,...,1\}$, which subjects to the condition $\sum_{j=1}^{m}\lambda_j^i=1$ for all $j=1,2,...,m$ and $i=1,2,...,N$ (m and N are the number of objectives and the population size, respectively).

Regarding the decomposition approaches (or scalarizing functions), there are three mainly used methods (namely weighted sum, Tchebycheff, and penalty-based boundary intersection functions) introduced in original MOEA/D [15]. Assume that $z^*=\left(z_1^*,z_2^*,...,z_m^*\right)^T$ is an ideal point, where its element z_j^* is always set to be the smallest f_j value found so far for all $j=1,2,...,m$. Each weight vector $\lambda^i=\left(\lambda_1^i,\lambda_2^i,...,\lambda_m^i\right)^T$ defines ith subproblem and its particular search direction $(i=1,2,...,N)$.

The definitions of these three methods are introduced below.

1) *Weighted Sum Approach* (*WS*) and *Tchebycheff Approach* (*TCH*)

These two methods (*WS* and *TCH*) are derived from the family of the L_p scalarizing functions ($p \geq 1$), as follows.

$$\text{Minimize} \quad g^{L_p}\left(x|\lambda^i,z^*\right)=\left(\sum_{j=1}^{m}(\lambda_j^i|f_j(x)-z^*|)^p\right)^{1/p} \tag{2}$$

$$\text{Subject to} \quad x\in\Omega.$$

WS and *TCH* are two extreme cases of $g^{L_p}\left(x|\lambda^i,z^*\right)$ with $p=1$ and $p=\infty$, respectively. Thus, the scalarizing functions of *WS* and *TCH* can be respectively defined by $g^{ws}\left(x|\lambda^i,z^*\right)=g^{L_1}\left(x|\lambda^i,z^*\right)$ and $g^{tch}\left(x|\lambda^i,z^*\right)=g^{L_\infty}\left(x|\lambda^i,z^*\right)$. To have a better understanding, the search direction of *WS* is illustrated in **Fig. 1(a)**, where the particular direction vector r^i of *i*th subproblem is set the same with the weight vector λ^i and the solutions located in the improvement region (*IR*) are better than the solution x^i. As pointed out in [5], *WS* puts more attentions to the solutions' convergence and has a better performance on the MOPs with convex PFs, but it gives a worse performance on the population's diversity when handling the MOPs with nonconvex PFs. Moreover, as shown in **Fig. 1(b)**, *TCH* gives more emphasis on the population's diversity, which is suitable to tackle the MOPs with nonconvex PFs when compared to *WS*. Especially, in *TCH*, $1/\lambda_j^i$ is used to replace λ_j^i in order to obtain a set of even distribution on search directions. In this case, λ_j^i is re-set to 10^{-5} when its value is 0, so as to guarantee the validity of the division [37].

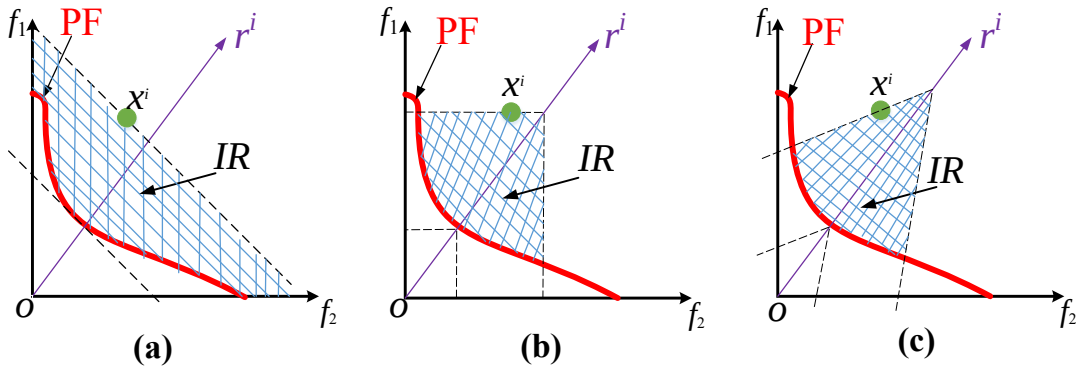

Fig. 1: Illustrations of three scalarizing functions with direction vector r^i using **(a)** *WS*, **(b)** *TCH*, **(c)** *PBI*, where dashed lines are contour lines and grid regions are the improvement region (*IR*) for the solution x^i.

2) *Penalty-Based Boundary Intersection Approach* (*PBI*)

PBI is a balanceable scalarizing function, which consists of two components, i.e., a convergence distance d_1^i and a diversity distance d_2^i. Here, as shown in **Fig. 2**, d_1^i is the projection distance of $F\left(x^i\right)-z^*$ on the weight vector λ^i, and d_2^i is the perpendicular distance between $F(x^i)$ and λ^i.

Then, the weights of these two distances are controlled by a user-defined penalty parameter θ, which tends to balance the convergence and the diversity for the population. Using mathematical format, *PBI* can be used to define the *i*th subproblem, as follows.

$$\text{Minimize} \quad g^{pbi}\left(x|\lambda^i,z^*\right)=d_1^i+\theta d_2^i \tag{3}$$

$$\text{where} \quad d_1^i=\left(F(x)-z^*\right)^T\lambda^i/\left\|\lambda^i\right\|, \quad d_2^i=\left\|F(x)-z^*-\left(d_1^i/\left\|\lambda^i\right\|\right)\lambda^i\right\|$$

$$\text{Subject to} \quad x\in\Omega.$$

Figure 1 (c) gives an illustration to show the search direction of *PBI*, and its direction vectors are the same with the preset weight vectors. By properly adjusting the parameter θ, *PBI* can well solve the MOPs with convex or nonconvex PFs. It is obvious that a small θ value can be set to prefer the convergence speed, while a large θ value tends to emphasize the population's diversity.

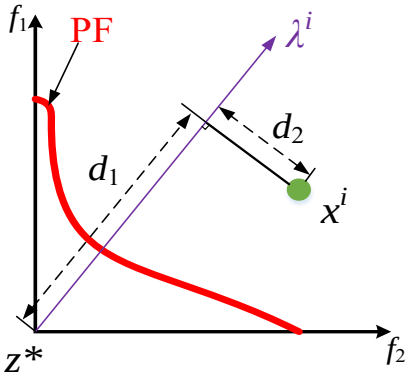

Fig. 2: The illustration of the projection distance and the perpendicular distance regarding the weight vector λ^i

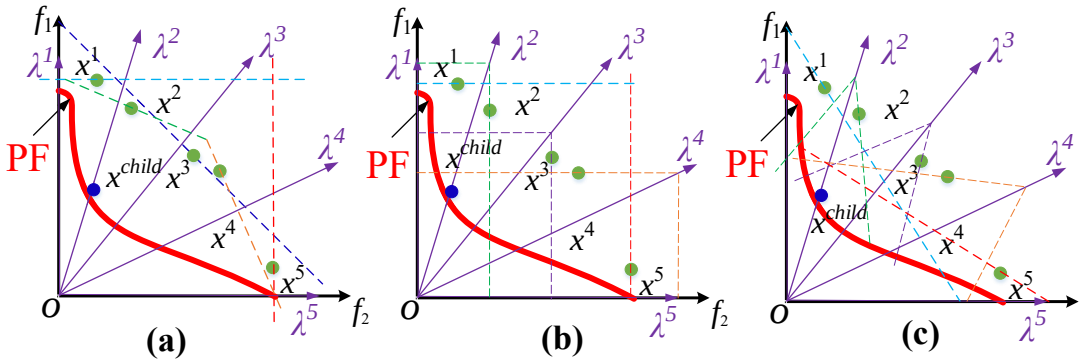

Fig. 3: Illustrations of the most serious cases of three scalarizing functions **(a)** *WS*, **(b)** *TCH*, **(c)** *PBI*

2.2 Constrained decomposition strategy

As shown in **Fig. 1**, the *IRs* for one solution may be too large for some problems with irregular PFs in MOEA/D [26], which results in the fact that several parent solutions from different subproblems may be substituted by a single new offspring solution and thus deteriorating the population's diversity.

Figure 3 illustrates the most serious cases that **(a)** *WS*, **(b)** *TCH* and **(c)** *PBI* are all going to be trapped in a local region. In each sub-plot of **Fig. 3**, there are five evenly distributed weight vectors $(\lambda^1,\lambda^2,\lambda^3,\lambda^4,\lambda^5)$ associated with five corresponding parent solutions (x^1,x^2,x^3,x^4,x^5). However, all of these five parent solutions will be replaced by a single new offspring solution x^{child}, as the solution x^{child} nearly falls on the true PF and all parent solutions' *IRs* contain x^{child}. In this way, the search process may be easily trapped in a local PF and the populations' diversity will be seriously lost. Thus, in order to alleviate the above-mentioned situation, a constrained decomposition strategy was proposed in [43], embedding constraints to the subproblems and reducing the volumes of *IRs* to control the balance of convergence and diversity. This way, the *i*th subproblem with weight vector λ^i has a feasible region (*FR*) in the objective space, where solutions in this region are assigned with the aggregated objective value $g(x|\lambda^i,z^*)$ as defined in Eq. (2-3), while solutions outside the feasible region are set to ∞ as their aggregated function values. This indicates that the solutions in *FR* of each subproblem are always better than the ones outside it, and thus the *IRs* of the subproblems are restricted within the *FRs*. To get these *FRs* and correspondingly reduce the *IRs*, there are two main approaches to define the constrained optimization subproblems in MOEA/D, as introduced below.

1) *Angle-based approach* [43] [45] [46]

To reduce the *IR*s, this method introduces an angle θ^i to adaptively control the *FR* of the *i*th subproblem, $i=1,2,...,N$, which is defined as follows.

$$\begin{aligned} &\text{Minimize } g^{constrained-A}(x|\lambda^i,z^*) \\ &\text{Subject to } \langle r^i,F(x)-z^*\rangle \le 0.5\theta^i \text{ and } x\in\Omega \end{aligned} \tag{4}$$

where $g^{constrained-A}(x|\lambda^i,z^*)$ is the aggregated objective function (e.g., *WS*, *TCH*, or *PBI*) and r^i is the particular direction vector of *i*th subproblem determined by the used decomposition method, which has been introduced in **Section 2.1**. Then, $\langle r^i,F(s)-z^*\rangle$ indicates the acute angle of r^i and $F(s)-z^*$, and the *FR* of *i*th subproblem can be adaptively controlled by adjusting the parameter θ^i, where each subproblem has an unique θ value based on the adjustment strategy in [43]. To visually clarify this method, **Fig. 4** illustrates the *IR* for one solution x^i associated to the *i*th subproblem.

2) *Distance-based approach* [44] [55]

This approach is mathematically defined as follows.

$$\begin{aligned} &\text{Minimize } g^{constrained-D}(x|\lambda^i,z^*) \\ &\text{Subject to } \operatorname{argmin} distance(r,F(x)-z^*)=r^i \text{ and } x\in\Omega \end{aligned} \tag{5}$$

where $distance(r,F(x)-z^*)$ is the Euclidean distance from r to $F(x)-z^*$, and other components like $g^{constrained-D}(x|\lambda^i,z^*)$ and r^i are the same as defined in the above *angle-based approach*. Thus, the *FR* of *i*th subproblem is defined to have the minimum distance from $F(x)-z^*$ to the reference vector r^i, and the *IR* is restricted within the *FR*.

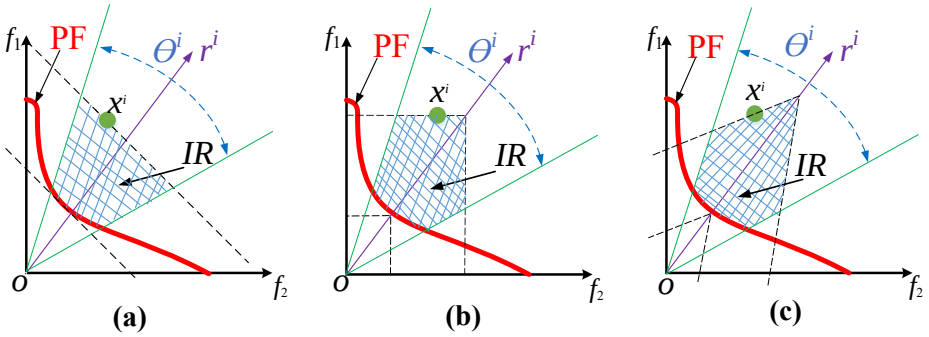

Fig. 4: Illustrations of the *IR*s for three constrained decomposition approaches using **(a)** *WS*, **(b)** *TCH*, **(c)** *PBI*, where dashed lines are contour lines and grid regions are the *IR*s for one solution x^i.

3. The Proposed MOEA/D-DDS Algorithm

In this section, the details of the proposed MOEA/D-DDS algorithm are introduced. At first, the framework of MOEA/D-DDS is provided, which gives an overview of our algorithm. Then, the two important procedures (offspring reproduction and the proposed DDS) are introduced. At last, an analysis related to the computational complexity of MOEA/D-DDS is given.

Algorithm 1 Framework of MOEA/D-DDS

Input: neighborhood size T, a mating selection control parameter δ, maximal generation G_{max}
Output: An approximation to the PF (PS)
1: Initialize population set $P\left(x^1,x^2,...,x^N\right)$, a set of weight vectors $\boldsymbol{W}\left(\lambda^1,\ \lambda^2,...,\lambda^N\right)$, generation G=1;
2: **While** G $\leq$ G_{max} **do**
3: $\boldsymbol{Q}$ = *Offspring_Reproduction* ($\boldsymbol{P}$, δ) //Introduced in **Section 3.2**
4: $\boldsymbol{R}$ = $\boldsymbol{P}$ + $\boldsymbol{Q}$ and set $\boldsymbol{P}=\varnothing$
5: $\boldsymbol{P}$ = *Dynamic_Decomposition_Strategy* ($\boldsymbol{R}$,$\boldsymbol{W}$) and G++ // Given in **Section 3.3**
6: **End While**
7: **Return** P

3.1 The Framework of MOEA/D-DDS

The proposed MOEA/D-DDS algorithm designs a dynamic decomposition strategy (DDS), which endeavors to well balance the diversity and the convergence during the evolution. To give an overview of MOEA/D-DDS, its framework is given in **Algorithm 1** with a very concise structure. First, in line 1 of **Algorithm 1**, a set of weight vectors $\left(\lambda^1,\lambda^2,...,\lambda^N\right)$ is evenly generated and the population $\boldsymbol{P}$ is randomly initialized with N solutions $\left(x^1,x^2,...,x^N\right)$ in the decision space. Second, the population $\boldsymbol{P}$ begins to evolve in lines 2-6 in order to search an approximation set until the stopping condition is satisfied, i.e., G reaches to G_{max}. When the evolution terminates, a set of solutions can be obtained, expecting to closely approximate to the true PF with even distribution. For each evolutionary cycle, the procedure of offspring reproduction is run, which has the neighborhood concept defining the adjacent solution vectors to run the restricted mating selection and the recombination operators (DE crossover

and polynomial-based mutation), and then an offspring population $\boldsymbol{Q}$ is generated in line 3. Details of this procedure will be given in **Section 3.2**. After that, the parent population $\boldsymbol{P}$ and the offspring population $\boldsymbol{Q}$ are combined as a union population $\boldsymbol{R}$ in line 4, and the proposed DDS is run on $\boldsymbol{R}$ to obtain the new population $\boldsymbol{P}$ in line 5. When compared to MOEA/D [15] and most of its variants [27] -[43], the main novelty of MOEA/D-DDS is the proposed DDS, which includes three main components, i.e., *distance-based* constrained decomposition approach, clustering-based dynamic decomposition approach and the convergence-based solution selection method (scalarizing functions in MOEA/D). With these three components, the proposed DDS strives to balance the convergence and the diversity for the population, the details of which are given in **Section 3.3.** At last, when the maximal generations are reached, the population $\boldsymbol{P}$ is outputted as an approximation set to the true PF in line 7.

3.2 Offspring reproduction

Reproduction is an important step to create an offspring population $\boldsymbol{Q}$, which includes three main procedures (mating selection, crossover and mutation). Each solution x^i in $\boldsymbol{P}$ needs several parent solutions to do reproduction. Generally, one solution is selected to run SBX [56], while two solutions are chosen to perform a DE variant (DE/rand/1) [30]. In these operators, mating selection plays an important role in the process of reproduction, as recombination of several distant or very different parents is disruptive and not likely to get superior offspring. Thus, the neighborhood information is used in our mating selection to restrictedly select mating parents from the neighboring subproblems with a high probability. As suggested in MOEA/D [15], the neighborhood information is defined to have T closest weight vectors as the neighbors of each weight vector. In this way, the neighbors of each subproblem are fixed at the beginning, in which the neighborhood information is heavily dependent on the used weight vectors. However, this approach may ignore the distribution of the population, and reduce the effect of recombination. To alleviate the above problem, T *angle-based* closest solutions to each solution x^i are defined in MOEA/D-DDS as its T neighbors $(i = 1, 2, ..., N)$. Here, the *angle* of solutions x^i and x^j can be computed by Eq. (6).

$$angle(x^i, x^j) \triangleq \arccos\left|\frac{\sum_{k=1}^{m} f_k(x^i)\cdot f_k(x^j)}{\sqrt{\sum_{k=1}^{m} f_k(x^i)^2}\cdot\sqrt{\sum_{k=1}^{m} f_k(x^j)^2}}\right| \tag{6}$$

where $f_k(x^i)$ is the kth objective value of x^i, $k \in \{1, 2, ..., m\}$ and m is the number of objectives.

To clearly show this procedure, **Algorithm 2** gives the details to produce the offspring population $\boldsymbol{Q}$, with the inputs $\boldsymbol{P}$ (the parent population) and δ (a parameter to control mating selection). First, in line 1, $\boldsymbol{Q}$ is initialized as an empty set. Then, the neighborhood information of x^i is obtained and preserved in $B(i)$, as shown in line 2, where $B(i)=\{i_1, i_2, ..., i_T\}$ indicating $(x^{i_1}, x^{i_2}, ..., x^{i_T})$ are T *angle-based* closest solutions to $x^i, i=(1,2,...,N)$. At last, an offspring population $\boldsymbol{Q}$ is obtained in lines

3-9 using the restricted mating selection and two recombination operators (DE crossover and polynomial-based mutation). Here, the restricted mating selection strategy and the recombination operators used in lines 4-7 are introduced. Based on the preset parameter δ and the neighborhood information of each solution x^i $i=(1,2,...,N)$, r_1 is randomly generated from [0,1] to set the mating selection index pool P_{ms} for x^i, as defined by

$$P_{ms}=\begin{cases} B(i) & \text{if } r_1<\delta, \\ (1,2,...,N) & \text{otherwise.} \end{cases} \tag{7}$$

Then, each element x_k^u $(k=1,2,...,n)$ in the new solution $x^u=(x_1^u,x_2^u,...,x_n^u)$ is generated by DE (n is the dimensions of the decision space), as follows.

$$x_k^u=\begin{cases} x_k^i+F\times(x_k^{i_d}-x_k^{i_h}) & \text{if } r_2<CR, \\ x_k^i & \text{otherwise.} \end{cases} \tag{8}$$

where CR is the crossover probability, F is the scaling factor, x^{i_d} and x^{i_h} are two selected parents from P_{ms}, and r_2 is randomly generated from [0,1]. Then, the polynomial-based mutation is further run on x^u to get a new offspring $x^v=(x_1^v,x_2^v,...,x_n^v)$ in line 7, as computed by

$$x_k^v=\begin{cases} x_k^u+\sigma_k\times(u_k-d_k) & \text{if } r_3<p_m, \\ x_k^u & \text{otherwise.} \end{cases} \tag{9}$$

$$\text{with } \sigma_k=\begin{cases} \left[2\times rd4+(1-2\times rd4)\times(1-\delta_1)^{(1+\eta)}\right]^{\frac{1}{\eta+1}}-1 & \text{if } r_4<0.5, \\ 1-\left[(2-2\times rd4)+(2\times rd4-1)\times(1-\delta_2)^{(1+\eta)}\right]^{\frac{1}{\eta+1}} & \text{otherwise} \end{cases} \tag{10}$$

$$\text{here } \delta_1=\frac{x_k^u-d_k}{u_k-d_k} \text{ and } \delta_2=\frac{u_k-x_k^u}{u_k-d_k}$$

where η is the distribution index, p_m is the mutation rate, r_3 and r_4 are both randomly generated from [0,1], while u_k and d_k are the upper and lower bounds of the kth decision variable, respectively.

Algorithm 2: *Offspring_Reproduction* (***P***, δ)

Input: ***P*** (a parent population) and δ (a control parameter for mating selection)
Output: The offspring population ***Q***

1: Initialize the offspring population $\boldsymbol{Q}=\varnothing$
2: Compute $B(i)=\{i_1\ldots i_T\}$ by finding T *angle-based* closest solutions to x^i ($i=1,2,...,N$)
3: **For** i = 1 to N **do**
4: Set mating selection index pool P_{ms} with Eq. (7)
5: Randomly select two indexes (i^d,i^h) from P_{ms} and get two parents (x^{i_d},x^{i_h}) from ***P***
6: Run DE crossover on x^{i_d}, x^{i_h} and x^i to get x^u
7: Run polynomial-based mutation on x^u to get x^v
8: Add x^v into Q
9: **End For**
10: **Return** Q

3.3 Dynamic decomposition strategy

As introduced in **Section 2**, a general decomposition approach transforms the MOP in Eq. (1) into a set of subproblems and thus the objective space of Eq. (1) is divided into a set of sub-regions (as shown in **Section 2.1**). A constrained decomposition strategy assigns each sub-region as the feasible region for the corresponding subproblem, and then the solutions in the feasible region of each subproblem are considered as the ones better than the outside ones, which have been introduced in **Section 2.2**. In the proposed DDS, a set of uniformly distributed weight vectors $\left(\lambda^1,\lambda^2,...,\lambda^N\right)$ is initially associated to the union population $\boldsymbol{R}$ (composed by the parent population $\boldsymbol{P}$ and the offspring population $\boldsymbol{Q}$), in which the *distance-based* constrained decomposition strategy defined in Eq. (5) is used to get N subsets $(S^1,S^2,...,S^N)$ with each S^i $(i=1,2,...,N)$ including the solutions falling into the feasible region of ith subproblem. In this process, each solution $x^i \in \boldsymbol{R}$ is associated to the closest weight vector by computing the distances of x^i and all the reference vectors in the objective space. Then, the distribution of $\boldsymbol{R}$ can be estimated by counting the number of solutions that fall within each feasible region, i.e., $n_i = \left|S^i\right|$ $(i = 1, 2, ..., N)$ with the constraint $\sum_{i=1}^{N} n_i = 2N$.

Algorithm 3 *Dynamic_Decompose* (S^i)

1: initialize $x^j \in S^i$ as a cluster C^j and cluster center cc^j, *size* = $|S^i|$, *flag*(C^j)=**false**
2: **while** *size* > 2
3: Find the two most closest clusters C^a and C^b subject to *flag*(C^a)= *flag*(C^b)=**false** by computing the *angles* between their centroids using Eq.(6)
4: Combine C^a and C^b as a new cluster C
5: Update the centroids of C using Eq. (11)
6: Set $C^a = C$ and *flag*(C^b)=**true**
7: *size*--
8: **end while**
9: **return** C^a, C^b subject to *flag*(C^a)= *flag*(C^b)=**false**

When tackling the general MOPs, it is often observed that some feasible regions are empty (i.e., $n_i = 0$), while other feasible regions overflow with many solutions (i.e., $n_i \geq 3$), especially at the begin of evolution. This is mainly because the preset weight vectors cannot always match the distribution of evolutionary population. To solve the above problem, the overflowed feasible regions should be further decomposed on a dynamic manner according to the population's distribution, which regenerates some new weigh vectors (i.e., subproblems) in order to substitute the empty weigh vectors (i.e., subproblems associated with no solutions). Thus, a clustering-based dynamic decomposition approach is designed to classify solutions in one most-crowded feasible region. In this paper, the agglomerative hierarchical clustering method [57] [58] is employed to explore the inner distribution and regularity of solutions in the most-crowded feasible region, so that the solutions in this region can be classified into two clusters

regarded as two subproblems. By this way, two new subproblems are re-generated from two clusters, by setting the centroids of two clusters as two weight vectors.

To further clarify the procedure of clustering-based dynamical decomposition, its pseudo-code is given in **Algorithm 3** with the input S^i (regarded as a cluster in this paper to preserve solutions in the feasible region of *i*th subproblem). This procedure aims to decompose S^i into two clusters (C^a, C^b) using the agglomerative hierarchical clustering method. Each solution $x^j \in S^i$ $(j = 1,2,...,|S^i|)$ is treated as one cluster and the centroid, as shown in line 1 of **Algorithm 3**, and we use *size* to represent the current number of clusters, which is initialized to $|S^i|$. Then, in lines 2-8, two most similar clusters are merged until only two clusters are left at last, i.e., *size*=2. In this process, the similarity of two different clusters is defined by computing the *angle* value using Eq. (6) between two clusters' centroids in line 3. In addition, once a new cluster *C* is generated, it needs to update the centroid in line 5 by computing the average vector of all the solutions in *C*. The cluster center *cc* of *C* can be computed by

$$f_i(cc) = \frac{\sum_{k=1}^{|C|} f_i(x^k)}{|C|} \tag{11}$$

where $x^k \in C$ and $i = 1, 2, \ldots m$. The centers of C^a, C^b can be treated as two weight vectors for new subproblems. After that, the *size* is reduced by 1 in line 7. While *size* is larger than 2, the above procedures in lines 3-7 will be run iteratively.

Algorithm 4 *Dynamic_Decomposition_Strategy*(***R***, *W*)

1: Apply *distance-based* constrained decomposition strategy to decompose ***R*** into *N* solution sets $(S^1, S^2, ..., S^N)$
2: Compute $T_{\max}$ by Eq. (12)
3: **For** i = 1 to $T_{\max}$ **do**
4: Find the cluster $S^t \in (S^1, S^2, ..., S^N)$ with the largest number of solutions
5: (S^x, S^y) = ***Dynamic_Decompose*** (S^t) //(**Algorithm 3**)
6: **Set** $S^t = S^x$ and $S^e = S^y$ (S^e is an empty cluster, $e \in (1,2,...,N) \cap n_e = 0$)
7: **End for**
8: Add a solution $x \in S^i, i \in (1,2,...,N)$ with a best value of *Convergence*(*x*) by Eq.(14) into ***P***
9: **Return *P***

With the above **Algorithm 3**, **Algorithm 4** is provided to clearly introduce the designed DDS. The detailed process is summarized as follows. Firstly, the *distance-based* constrained decomposition strategy is applied to decompose ***R*** into *N* solution sets $(S^1, S^2, ..., S^N)$ in line 1 of **Algorithm 4** based on the preset weight vectors $(\lambda^1, \lambda^2, ..., \lambda^N)$. Here, S^i saves the solutions falling into the *i*th subproblem's feasible region and n_i is used to record its size, i.e., $n_i = |S^i|$ with $i = 1,2,...,N$ (*N* is number of weight vectors). The total number of empty feasible regions (with $n_i = 0$) is obtained in line 2, which is recorded by $T_{\max}$ in Eqs. (12)-(13).

$$T_{\max} = \sum_{i=1}^{N} E_i \tag{12}$$

$$\text{with}\quad E_i=\begin{cases}1 & \text{if } n_i=0\\ 0 & \text{if } n_i\neq 0\end{cases},\quad i=1,2,...,N \tag{13}$$

This value of $T_{\max}$ also indicates the number of times to do the clustering-based dynamic decomposition. Next, this process of dynamic decomposition is run to replace the empty subproblems in lines 3-7. In this process, **Algorithm 3** is adopted to iteratively divide the cluster S^t with the maximum record size $n_t=\max\{n_i\}$ $(i=1,2,...,N)$ into two new clusters (S^x,S^y) in lines 4-5. Please note that when there are more than one subproblem associated with the largest number of solutions, one of them will be randomly selected. Then, the replacement of subproblems is run, by using S^x to replace S^t and using S^y to update one empty cluster in line 6. At last, N subproblems whose feasible regions having at least one solution can be obtained and a simple convergence indicator in Eq. (14) is used to select only one best solution from each feasible region into $\boldsymbol{P}$ in line 8. Here, $Convergence(x^i)$ indicates the convergence performance for solution x^i, as defined by

$$Convergence(x^i)=\sum_{j=1}^{m} f_j(x^i) \tag{14}$$

In order to facilitate the understanding of our proposed DDS, a simple example is given in **Fig. 5**. As shown in **Fig. 5(a)**, four preset weight vectors ($\lambda^1,\lambda^2,\lambda^3,\lambda^4$) are distributed uniformly in the objective space and they separate the bi-objective space into four feasible sub-regions (L_1, L_2, and L_3 are the boundary lines of the feasible sub-regions). In this example, the union population $\boldsymbol{R}$ includes eight solutions (*a*, *b*, *c*, *d*, *e*, *f*, *g*, and *h*) in the bi-objective space. First, as shown in **Fig. 5(a)**, *distance-based* constrained decomposition strategy is used to obtain four solution sets (S^1,S^2,S^3,S^4), where *a* and *b* belong to S^1; *c*, *d*, *e*, *f*, and *g* are associated to S^3; *h* falls into S^4, while S^2 has no associated solution. As S^3 has the largest number of associated solutions, **Algorithm 3** is run on it to get two new clusters, in which *c* and *d* belong to one cluster, while *e*, *f*, and *g* are collected into other cluster. At last, one solution is selected by Eq. (14) in each cluster to have a better convergence, which is marked by red color in **Fig. 5(b)**.

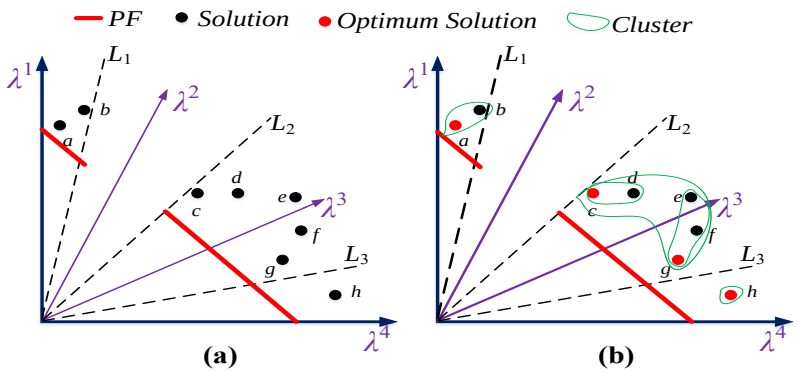

Fig. 5 A simple example to show the process of dynamic decomposition strategy.

3.4 Computational Complexity of MOEA/D-DDS

As introduced in **Section 3.1**, MOEA/D-DDS includes two main produces, i.e., offspring reproduction (mating selection and recombination operators) and the proposed DDS (environmental selection), which determine the computational complexity of MOEA/D-DDS in one generation. As shown in **Algorithm 1**, it requires a time complexity of $O(mN^2)$ (m is the number of objectives and N is the population size) to get the offspring population $\boldsymbol{Q}$ in line 3. The details of this process are given in **Algorithm 2**, where the computational complexity is mainly dominated by the process of preserving the neighbor information of each solution in line 2. Regarding the proposed DDS, in line 5 of **Algorithm 1** (details are given in **Algorithm 4**), it needs a time complexity of $O(mN^2)$ to run the *distance-based* constrained decomposition strategy to decompose the union population $\boldsymbol{R}$ into N clusters $(S^1, S^2, ..., S^N)$ with the set of weight vectors (in line 1 of **Algorithm 4**). In the loop of dynamic decomposition to re-generate new subproblems in lines 3-7 of **Algorithm 4**, the time complexity is mainly determined by the clustering-based method (**Algorithm 3**) in line 5, which requires a time complexity of $O\left(m|S^i|^2\right)$ to divide the input population S^i into two new cluster ($|S^i|$ indicate the cardinality of S^i, and S^i is regarded as a cluster in this paper to preserve solutions in the feasible region of ith subproblem). In the experimental studies, we find that $|S^i| \ll N$ for most considered MOPs, especially in the last stage of evolution. However, there is the worst scenario that all solutions in $\boldsymbol{R}$ are clustered in the same feasible region of ith subproblem (i.e., $|S^i|=2N$ and the $T_{\max}=N-1$ in line 2 of **Algorithm 4**), it needs a worst time complexity of $O\left(m\sum_{i=1}^{T_{\max}}|S^i|^2\right) \approx O(mN^3)$ to finish the loop in the DDS. Especially, the cardinality of S^i becomes smaller with the running of clustering. Therefore, considering the above computational complexity analysis of all the procedures, the overall worst time complexity of MOEA/D-DDS is approximated to $O(mN^2)+O\left(m\sum_{i=1}^{T_{\max}}|S^i|^2\right)$ $\approx O(mN^3)$ in one generation.

4. The Experimental Studies

In this section, six competitive MOEAs, i.e., NSGA-III [55], MOEA/D-DE [30], MOEA/D-DRA [27], MOEA/D-STM [37], MOEA/D-IR [41], and MOEA/D-ACD [43], are adopted here to study the performance of the proposed MOEA/D-DDS algorithm. Twenty-six various MOPs, i.e., WFG1-WFG9 [59], UF1-UF10 [60], and MOP1-MOP7 [25], are considered here as the test problems to run the empirical studies. To access the quality of solutions obtained by these compared MOEAs, two widely used performance metrics are employed in our experiments, such as inverted generational distance (IGD) [64] and hyper-volume (HV) [17]. In the following subsections, the experimental studies are divided into the three main components. Firstly, some information related to the compared MOEAs, the considered test problems, the parameters settings and the used performance metrics (IGD and HV), are introduced. Then, the experimental studies about the proposed MOEA/D-DDS are given. Finally, more

discussions about DDS are provided to show its advantages.

4.1 Related Experimental Information

4.1.1 Compared MOEAs

Six competitive MOEAs are used here to testify the performance of our proposed MOEA/D-DDS, which are briefly introduced below.

1). NSGA-III [55]: It was an enhanced version of NSGA-II to tackle many objective optimization problems. In NSGA-III, using the preset uniformly distributed reference vectors, the *distance-based* constrained decomposition strategy is used to design a niche method, which assigns each solution to the nearest reference line. In the feasible region of reference line, when multiple solutions have the best non-dominated sorting rank, one solution with the shortest distance to the reference line is selected for next generation. Under this way, NSGA-III tries to alleviate the loss of selection pressure by enhancing diversity management using the *distance-based* constrained decomposition strategy.

2). MOEA/D-DE [30]: In order to solve some complicated MOPs with variable dependencies, differential evolution (DE) operator are employed in MOEA/D to substitute its original crossover operator (SBX).

3). MOEA/D-DRA [27]: In the competition of MOEAs in CEC2009, this algorithm showed the superior performance on tackling most of the complicated MOPs. A dynamic resource allocation strategy was proposed in MOEA/D-DRA, which computes the utility function for each subproblem and dynamically selects the subproblems having high potentiality to be improved.

4). MOEA/D-STM [37]: It adopts a stable matching model (STM) to associate the subproblems and the solutions, aiming to balance the convergence and the diversity for the population during the evolutionary process.

5). MOEA/D-IR [41]: This algorithm is enhanced from MOEA/D-STM. An inter-relationship model was presented to associate solutions based on the principle of diversity first and convergence second, which considers the mutual-preferences of the subproblems and the solutions.

6). MOEA/D-ACD [43]: It is a recently proposed MOEA/D variant, which designs an adaptive *angle-based* constrained decomposition approach to enhance the population's diversity.

4.1.2 Benchmark Problems

In our experiments, twenty-six various unconstrained MOPs are considered here to assess the performance of the proposed MOEA/D-DDS algorithm, and their features are briefly introduced below.

UF1-UF10 are initially proposed as the benchmark problems for the competition of MOEAs in CEC2009 [60], which show very complicated PSs in the search space. For MOP1 to MOP7 [25], they are modified from ZDT [61] and DTLZ [62] problems, characterized with various twisted search landscapes, in which the solution in a tiny search area can dominate other solutions in the large area. Thus, to avoid the trap in local area of a MOEA, it is important to maintain the diversity when solving

MOP1-MOP7. Considering the WFG test problems (WFG1-WFG9) [59], they are characterized with various complex features, such as non-separable, deceptive, degenerate, variable dependent, different scaled and mixed PF shapes.

According to the number of objectives (summarized in **Table 1**), UF1-UF7 and MOP1-MOP5 are two-objective problems, while UF8-UF10 and MOP6-MOP7 are three-objective problems. More importantly, WFG1-WFG9 can be scalable to any number of objectives and they are scaled to three-objective problems in this paper. In addition, the numbers of decision variables of UF1-UF10 and MOP1-MOP7 are respectively set to 30 and 10; Especially for WFG1-WFG9, they have position- and distance-related decision variables, whose numbers are respectively set to 4 and 10. More information above these test problems can be found in [25], [59], and [60].

4.1.3 Performance Indicators

In this paper, to evaluate the performance among the compared algorithms, two widely used performance indicators are used in our empirical studies, i.e., the inverted generational distance (IGD) [64] and the Hyper-volume (HV) [17], which can simultaneously reflect the quality of solutions obtained by different MOEAs, on the aspects of convergence and diversity.

Table 1 Basic settings of IGD and HV for different test problems

Problems	Numbers of Objectives (m)	Numbers of Sampling Points in P^*	Reference Points z^r
WFG1-WFG9	3	2000	(3.0,5.0,7.0)
UF1-UF7	2	1000	(2.0,2.0)
UF8-UF10	3	10000	(2.0,2.0,2.0)
MOP1-MOP5	2	5000	(2.0,2.0)
MOP6-MOP7	3	5000	(2.0,2.0,2.0)

1). IGD: assuming that S is a set of optimum solutions obtained by a MOEA, the IGD indicator is designed to compute the average distance from a subset of true PF to S, which can simultaneously show the convergence and the distribution of S along the true PF. Thus, when computing the IGD indicator, the information about the true PF of the underlying MOP should be known in advance. Generally, a uniformly sampled set (P^*) from the true PF is used to calculate the IGD value of S, as follows.

$$IGD(S,P^*)=\frac{\sum_{i=1}^{|P^*|}\min_{j=1}^{|S|} dist(p^i,x^j)}{|P^*|} \tag{15}$$

where $dist(p^i,x^j)$ indicates the Euclidean distance between a solution $p^i\in P^*$ and a solution $x^j\in S$. $|P^*|$ and $|S|$ respectively indicate the number of solutions in P^* and S. It is noted that the set S with a low IGD value indicates the high approximation to the entire PF. Moreover, the numbers of points ($|P^*|$) on the true PF should be as larger as possible in order to improve the computational accuracy. In our empirical studies, the sizes of $|P^*|$ for different test problems are given in **Table 1.**

2). HV: assuming that S is a set of solutions obtained by a MOEA, the HV indicator is designed to compute the volume of the dominated objective space of S in a limited space. Generally, the nadir point of the true PF, i.e., a reference point $z^r = (z_1^r, ..., z_m^r)^T$, is defined as the bound of the limited space, in order to get the HV value. As suggested in [41], each element in z^r should be set slightly bigger than the corresponding value of the nadir point. Then, the HV metric can be calculated as follows.

$$HV(S) = \mathrm{Vol}(\bigcup_{x \in S} [f_1(x), z_1^r] \times ... [f_m(x), z_m^r]) \tag{16}$$

where $\mathrm{Vol}(\cdot)$ denotes the Lebesgue measure. When calculating the HV value, the solutions in S that cannot dominate z^r will be discarded (i.e., solutions in S that cannot dominate z^r are not included to compute HV). Similar to [41], an integer larger than the member of the nadir point in each objective is adopted in our experiments as the reference point, which is shown in **Table 1** for different test problems. Generally, the solution set S with a larger HV value indicates a more promising performance to approach the true PF.

4.2 Experimental Parameter Settings

MOEA/D-DE, MOEA/D-DRA, MOEA/D-STM, MOEA/D-IR, MOEA/D-ACD and the proposed MOEA/D-DDS are designed based on the decomposition approach, which employ the DE crossover operator for reproduction, while NSGA-III applies the SBX crossover operator and its parameters are set as suggested in [55]. The detailed parameter settings of these decomposition-based MOEAs are summarized in **Table 2**.

Table 2 General Experimental Parameter Settings

Basis Setting types	Parameter Settings
Reproduction operators	Mutation probability $p_m = 1/n$,
	Distribution index $u_m = 20$
	CR=0.5 and F=0.5 for WFG; CR=1.0 and F=0.5 for UF and MOP [41]
Population Size (N)	N=600 for UF1 to UF7; N=1000 for UF8 to UF10; N=100 for MOP1 to MOP5; N=300 for MOP6 and MOP7; N=300 for WFG1 to WFG9
Number of Runtimes	Each algorithm is independently launched 30 times on each test problems
Function Evaluations	300 000 for UF and MOP problems and 120 000 for WFG problems
Neighborhood Size (T)	T=15 for bi-objective problems and T=20 for three-objective problems
Probability (δ)	δ=0.9 for all the decomposition-based MOEAs

In Table 2, δ is a user-defined parameter to control the restricted mating selection in MOEAs; CR and F are two parameters to control the DE crossover operator [65]. To have a fair comparison with all the compared algorithms, we actually use the same parameter settings from their references. Due to the different difficulties for different kinds of problems, the compared algorithms usually will adopt different values of parameters (CR, F, N) for comparison, in order to guarantee that most of the compared algorithms can be well converged, which will have a reasonable and justified comparison. Additionally, all the compared MOEAs in this paper are implemented in JAVA. The source code of NSGA-III was implemented by the authors of θ-DEA [66], while the other source codes are provided

by their authors.

4.3 Comparison with Several Competitive MOEAs

In this section, MOEA/D-DDS is compared to NSGA-III, MOEA/D-DE, MOEA/D-DRA, MOEA/D-STM, MOEA/D-IR and MOEA/D-ACD on twenty-six test problems (WFG1-WFG9, UF1-UF10, and MOP1-MOP7). After obtaining the IGD and HV results, Wilcoxon rank sum test was further run with a significance level α =0.05 to get a statistically sound conclusion, which shows the statistically significant differences between the results of MOEA/D-DDS and other MOEAs. In the following tables, all the IGD and HV results obtained by each MOEA are expressed in terms of $Mean(Std)$ for each test MOP, where *Mean* and *Std* are respectively the mean value and the standard deviation value from 30 run. The symbols "+", "–", and "~" indicate that the results of other MOEAs are respectively better than, worse than, and similar to the ones of MOEA/D-DDS, under Wilcoxon rank sum test. Please note that the best mean result of each test MOP is highlighted with boldface in gray background for easy observation.

4.3.1 Comparison on WFG1-WFG9

All the performance comparisons of seven MOEAs on WFG1-WFG9 are given in **Tables 3** and **4**, which respectively list the IGD and HV results. These experimental results show that MOEA/D-DDS has a promising performance in solving WFG problems, as it is best on 3 out of 9 cases both on IGD and HV. By contrast, NSGA-III, MOEA/D-DE, MOEA/D-DRA, MOEA/D-STM, MOEA/D-IR and MOEA/D-ACD are respectively best on 4, 0, 1, 0, 0 and 1 cases for IGD and respectively best on 3, 0, 0, 1, 1, and 1 cases for HV, as summarized in the second last row of **Tables 3** and **4**. In the last row of **Tables 3** and **4**, the comparison summary of MOEA/D-DDS with each of other MOEAs is given when considering all the WFG problems, where "+/–/~" give the total number of test problems on which the corresponding MOEA performs better than, worse than, and similarly to MOEA/D-DDS.

Table 3 Performance Comparisons of IGD on WFG1-WFG9 Test Problems

Problem	NSGA-III	MOEA/D-DE	MOEA/D-DRA	MOEA/D-STM	MOEA/D-IR	MOEA/D-ACD	MOEA/D-DDS
WFG1	8.13E-01(1.84E-01)+	1.10E+00(6.92E-02)~	9.02E-01(8.10E-02)+	7.27E-01(1.39E-01)+	7.12E-01(1.35E-01)+	**3.92E-01(4.30E-02)+**	1.14E+00(1.18E-02)
WFG2	**1.26E-01(8.14E-03)+**	3.98E-01(3.28E-02)–	4.06E-01(3.57E-02)–	3.32E-01(6.47E-02)–	3.05E-01(6.82E-02)–	3.07E-01(6.86E-02)–	1.90E-01(4.28E-02)
WFG3	5.49E-02(4.43E-03)+	3.89E-02(6.86E-04)+	**3.75E-02(7.06E-04)+**	4.25E-02(3.34E-04)+	4.74E-02(1.60E-03)+	4.13E-02(1.28E-03)+	1.36E-01(7.10E-03)
WFG4	**9.80E-02(8.18E-04)+**	2.07E-01(4.21E-03)–	2.04E-01(4.26E-03)–	1.71E-01(7.09E-03)–	1.65E-01(7.14E-03)–	1.67E-01(7.50E-03)–	1.48E-01(1.99E-03)
WFG5	**1.42E-01(1.20E-03)+**	1.93E-01(1.79E-03)–	1.94E-01(1.89E-03)–	1.67E-01(1.24E-03)–	1.64E-01(1.45E-03)–	1.67E-01(5.83E-04)–	1.48E-01(1.01E-03)
WFG6	1.57E-01(1.08E-02)–	2.30E-01(6.12E-02)–	2.48E-01(6.93E-02)–	1.62E-01(2.60E-02)–	1.60E-01(1.19E-02)–	2.00E-01(6.00E-02)–	**1.32E-01(3.92E-03)**
WFG7	**1.12E-01(1.55E-04)+**	1.71E-01(1.14E-03)–	1.70E-01(1.28E-03)–	1.42E-01(9.07E-04)–	1.40E-01(1.35E-03)–	1.41E-01(1.15E-03)–	1.27E-01(1.14E-03)
WFG8	2.68E-01(4.33E-03)–	2.94E-01(1.18E-02)–	2.90E-01(1.49E-02)–	2.78E-01(8.26E-03)–	2.61E-01(9.90E-03)–	2.73E-01(1.18E-02)–	**2.30E-01(3.75E-03)**
WFG9	1.33E-01(1.02E-03)–	1.94E-01(3.91E-02)–	2.19E-01(6.65E-02)–	1.76E-01(5.86E-02)–	1.60E-01(4.00E-02)–	1.78E-01(5.39E-02)–	**1.28E-01(3.27E-02)**
Best/All	**4/9**	**0/9**	**1/9**	**0/9**	**0/9**	**1/9**	**3/9**
+/–/~	**6/3/0**	**1/7/1**	**2/7/0**	**2/7/0**	**2/7/0**	**2/7/0**	———

When compared to MOEA/D-DE and MOEA/D-DRA, MOEA/D-DDS has shown an absolute advantage, as it outperforms them on 7 test problems regarding IGD and on 6 test problems regarding

HV; whereas, MOEA/D-DE and MOEA/D-DRA outperform MOEA/D-DDS on WFG1 and WFG3, when considering both of IGD and HV. To be specific, as WFG1 has a convex, mixed and biased PF, while WFG3 owns a linear and unimodal PF, MOEA/D-DDS is not so good at solving WFG1 and WFG3. Regarding the comparisons to MOEA/D-STM, MOEA/D-IR, and MOEA/D-ACD, MOEA/D-DDS also shows some advantages, as it outperforms them on at least 5 test problems. Except for WFG1 and WFG3, MOEA/D-DDS performs better on most cases when considering both of IGD and HV. MOEA/D-DDS only performs worse than MOEA/D-IR and MOEA/D-ACD on WFG2 regarding IGD and HV, and similarly to MOEA/D-STM on WFG2 and WFG4 regarding HV. For WFG4-WFG9 with concave PFs, MOEA/D-DDS shows superior performance over other decomposition-based competitors. Since a complicated normalization procedure is used in NSGA-III to compute the intercepts along each objective axis, which helps to eliminate the impact of different amplitudes on multiple objectives for WFG1-WFG9, NSGA-III can give the best results on most cases of WFG problems regarding IGD and HV. MOEA/D-DDS performs a little worse than NSGA-III, as it is only better than NSGA-III on three test problems (WFG6, WFG8, and WFG9).

Table 4 Performance Comparisons of HV on WFG1-WFG9 Test Problems

Problem	NSGA-III	MOEA/D-DE	MOEA/D-DRA	MOEA/D-STM	MOEA/D-IR	MOEA/D-ACD	MOEA/D-DDS
WFG1	8.12E+01(3.90E+00)+	5.71E+01(2.44E+00)+	6.47E+01(3.27E+00)+	7.14E+01(5.93E+00)+	7.25E+01(5.72E+00)+	**8.90E+01(2.08E+00)+**	5.65E+01(2.88E-01)
WFG2	9.99E+01(3.95E+00)~	9.97E+01(2.76E-01)~	9.98E+01(1.87E-01)~	9.97E+01(4.58E-01)~	**1.00E+02(2.30E-01)+**	1.00E+02(5.01E-01)+	9.97E+01(2.67E-01)
WFG3	7.53E+01(2.40E-01)+	7.61E+01(1.95E-02)+	7.61E+01(3.15E-02)+	**7.61E+01(5.14E-03)+**	7.60E+01(1.77E-02)+	7.61E+01(2.24E-02)+	7.16E+01(5.52E-01)
WFG4	**7.76E+01(6.94E-02)+**	7.53E+01(1.98E-01)–	7.58E+01(1.43E-01)–	7.59E+01(2.17E-01)~	7.62E+01(1.73E-01)~	7.55E+01(3.03E-01)–	7.60E+01(1.20E-01)
WFG5	**7.39E+01(3.76E-01)+**	7.18E+01(1.34E-01)–	7.20E+01(1.25E-01)–	7.19E+01(1.61E-01)–	7.27E+01(2.21E-01)–	7.19E+01(1.68E-01)–	7.32E+01(1.89E-01)
WFG6	7.32E+01(7.36E-01)–	7.22E+01(4.63E+00)–	7.10E+01(5.30E+00)–	7.61E+01(2.06E+00)–	7.58E+01(1.18E+00)–	7.27E+01(4.41E+00)–	**7.66E+01(3.89E-01)**
WFG7	**7.79E+01(3.81E-02)+**	7.62E+01(1.62E-01)–	7.64E+01(1.42E-01)–	7.65E+01(3.02E-01)–	7.70E+01(8.87E-02)–	7.70E+01(3.67E-01)–	7.71E+01(7.62E-02)
WFG8	6.66E+01(2.59E-01)–	6.75E+01(1.27E+00)–	6.76E+01(1.36E+00)–	6.70E+01(2.05E-01)–	6.82E+01(1.28E+00)–	6.75E+01(9.10E-01)–	**6.89E+01(1.18E-01)**
WFG9	7.32E+01(1.49E-01)–	7.20E+01(2.76E+00)–	7.03E+01(4.76E+00)–	7.14E+01(3.87E+00)–	7.28E+01(2.66E+00)–	7.13E+01(3.44E+00)–	**7.35E+01(1.96E+00)**
Best/All	**3/9**	**0/9**	**0/9**	**1/9**	**1/9**	**1/9**	**3/9**
+/–/~	**5/3/1**	**2/6/1**	**2/6/1**	**2/5/2**	**3/5/1**	**3/6/0**	———

Therefore, when compared to decomposition-based MOEAs, it is reasonable to draw a conclusion that the proposed MOEA/D-DDS presents a superior performance over MOEA/D-DE, MOEA/D-DRA, MOEA/D-STM, MOEA/D-IR and MOEA/D-ACD with respect to IGD and HV on all the WFG problems. As introduced in **Section 3.1**, the main novelty of MOEA/D-DDS is the proposed DDS when compared to the above decomposition-based MOEAs. The superior performance of MOEA/D-DDS on these WFG test problems indicates the advantages of our proposed DDS, which can regenerate the weight vectors to fit the evolutionary population.

4.3.2 Comparison Results on UF1-UF10

The mean IGD and HV results of seven MOEAs on UF1-UF10 problems are reported in **Table 5** and

Table 6, respectively. It can be observed that MOEA/D-DDS obtains significantly better results for 4 out of 10 cases both on IGD and HV, while NSGA-III, MOEA/D-DE, MOEA/D-DRA, MOEA/D-STM, MOEA/D-IR and MOEA/D-ACD are best on 3, 0, 0, 1, 2 and 0 cases for IGD and best on 2, 0, 0, 1, 3, and 0 cases for HV, respectively. The comparison summary of MOEA/D-DDS with each algorithm on UF problems is listed in the last row of **Table 5** and **Table 6**, respectively for IGD and HV.

Table 5 Performance Comparisons of IGD Values on UF1-UF10 Test Problems

Problem	NSGA-III	MOEA/D-DE	MOEA/D-DRA	MOEA/D-STM	MOEA/D-IR	MOEA/D-ACD	MOEA/D-DDS
UF1	9.43E-02(1.26E-02)–	1.07E-03(8.01E-05)–	2.27E-03(5.11E-04)–	1.04E-03(1.04E-04)–	1.12E-03(5.40E-05)~	1.06E-03(8.73E-05)–	**1.03E-03(7.81E-05)**
UF2	2.89E-02(2.72E-03)–	5.11E-03(1.90E-03)–	5.32E-03(2.42E-03)–	3.17E-03(1.67E-03)+	**2.69E-03(1.04E-03)+**	6.23E-03(9.48E-04)–	5.63E-03(1.35E-03)
UF3	2.01E-01(4.99E-02)–	2.43E-02(2.05E-02)–	1.82E-02(1.96E-02)–	8.14E-03(5.78E-03)–	9.16E-03(7.51E-03)–	2.88E-02(2.08E-02)–	**7.90E-03(2.74E-03)**
UF4	**4.24E-02(5.29E-04)+**	5.67E-02(3.50E-03)~	5.49E-02(4.74E-03)~	5.30E-02(2.97E-03)+	5.33E-02(3.61E-03)~	5.76E-02(4.58E-03)–	5.28E-02(2.99E-03)
UF5	**2.09E-01(3.98E-02)+**	3.22E-01(6.17E-02)~	2.97E-01(7.09E-02)~	2.48E-01(2.11E-02)–	2.64E-01(4.46E-02)~	4.16E-01(6.83E-02)–	2.70E-01(2.10E-02)
UF6	2.14E-01(7.03E-02)–	9.57E-02(5.73E-02)–	1.04E-01(5.47E-02)–	8.61E-02(4.11E-02)~	9.25E-02(4.20E-02)–	1.57E-01(1.52E-01)–	**7.38E-02(2.32E-02)**
UF7	7.80E-02(9.13E-02)–	1.86E-03(1.91E-03)+	1.93E-03(4.95E-04)+	**1.06E-03(6.38E-05)+**	1.14E-03(7.98E-05)+	1.80E-03(5.41E-04)+	3.58E-03(9.21E-04)
UF8	1.67E-01(2.60E-03)–	5.93E-02(9.56E-03)~	4.48E-02(1.23E-02)+	2.87E-02(3.50E-03)+	**2.61E-02(4.45E-03)+**	5.26E-02(8.93E-03)–	5.21E-02(8.24E-03)
UF9	1.65E-01(3.15E-02)–	6.07E-02(4.28E-02)–	5.89E-02(4.91E-02)–	3.74E-02(3.39E-03)–	3.14E-02(2.91E-02)–	1.02E-01(5.01E-02)–	**2.66E-02(5.70E-03)**
UF10	**2.29E-01(5.28E-02)+**	5.55E-01(6.32E-02)+	4.63E-01(4.74E-02)+	8.71E-01(2.04E-01)+	4.86E-01(6.72E-02)+	7.43E-01(9.58E-02)+	1.75E+00(2.53E-01)
Best/All	**3/10**	**0/10**	**0/10**	**1/10**	**2/10**	**0/10**	**4/10**
+/–/~	**3/7/0**	**2/5/3**	**3/5/2**	**5/4/1**	**4/3/3**	**2/8/0**	———

Table 6 Performance Comparisons of HV Values on UF1-UF10 Test Problems

Problem	NSGA-III	MOEA/D-DE	MOEA/D-DRA	MOEA/D-STM	MOEA/D-IR	MOEA/D-ACD	MOEA/D-DDS
UF1	3.386(8.31E-02)–	3.662(6.50E-04)–	3.657(3.65E-03)~	3.663(1.10E-03)–	3.662(9.65E-04)–	3.414(3.20E-01)–	**3.678(9.15E-04)**
UF2	3.576(2.34E-02)–	3.646(1.70E-02)~	3.649(1.31E-02)~	3.655(6.51E-03)+	**3.656(1.33E-02)~**	2.765(3.22E-01)–	3.647(8.84E-03)
UF3	2.798(1.13E-01)–	3.556(1.11E-01)–	3.591(1.20E-01)–	3.640(2.61E-02)–	3.637(2.67E-02)–	3.475(3.27E-01)–	**3.685(5.04E-02)**
UF4	**3.215(3.30E-03)+**	3.173(1.15E-02)–	3.161(2.17E-02)–	3.179(1.25E-02)~	3.087(7.14E-02)–	2.924(5.63E-02)–	3.182(1.29E-02)
UF5	2.742(1.55E-01)–	2.619(1.92E-01)–	2.646(2.03E-01)–	**2.928(6.18E-02)+**	2.716(2.88E-01)–	2.335(2.21E-01)–	2.887(5.94E-02)
UF6	2.809(2.06E-01)–	3.112(1.80E-01)–	3.087(1.72E-01)–	3.168(8.66E-02)–	3.023(2.58E-01)–	2.932(4.13E-01)–	**3.183(5.81E-02)**
UF7	3.262(3.10E-01)–	3.488(2.71E-02)~	3.493(4.01E-03)+	3.496(9.99E-04)+	**3.497(2.11E-03)+**	3.274(3.35E-01)–	3.488(3.14E-03)
UF8	6.421(1.18E-02)–	7.308(2.03E-02)–	7.331(2.91E-02)~	7.346(1.71E-02)~	**7.417(9.28E-03)+**	7.243(2.66E-02)–	7.321(1.99E-02)
UF9	6.216(2.81E-01)–	7.492(1.84E-01)–	7.527(2.12E-01)–	7.650(1.71E-02)–	7.709(1.35E-01)~	7.203(2.02E-01)–	**7.722(4.04E-02)**
UF10	**6.172(1.94E-01)+**	3.286(2.75E-01)+	3.671(2.68E-01)+	2.309(7.08E-01)+	3.606(4.29E-01)+	2.470(2.73E-01)+	0.214(2.93E-01)
Best/All	**2/10**	**0/10**	**0/10**	**1/10**	**3/10**	**0/10**	**4/10**
+/–/~	**2/8/0**	**1/7/2**	**2/5/3**	**4/4/2**	**3/5/2**	**1/9/0**	———

Specifically, when solving UF1 with a regular PF, only the IGD and HV results of NSGA-III on these three problems are significantly inferior to other algorithms. That is to say, except NSGA-III, the other six MOEAs perform well on UF1. Furthermore, for UF2 and UF7 having similar PFs with UF1, NSGA-III still shows the worst performance on them. For UF3 with a concave PF, MOEA/D-DDS has the best performance both for IGD and HV. Regarding UF4 as a difficult instance with concave PF in the objective space, NSGA-III obtains the best result, and MOEA/D-DDS performs better than other five decomposition-based MOEAs. With respect to UF5 and UF6 both with discontinuous PFs in the objective space, all these MOEAs are unable to approximate the entire UF, as both their IGD and HV

results are unsatisfactory. As shown in **Table 5** and **Table 6**, MOEA/D-DDS is better than other competitors on UF6. However, for UF5, NSGA-III has the best result on IGD, but has the inferior result on HV, while MOEA/D-STM is better than other competitors on HV. With respect to the three-objective instances UF8 and UF9 (UF9 is with two disconnected PFs), the results indicate that MOEA/D-IR is best among the compared MOEAs on UF8, while MOEA/D-DDS performs best on UF9. Since UF10 is an extension version of UF8 with a multimodal PF, all of these MOEAs fail to converge to the true PF, where NSGA-III performs the best while MOEA/D-DDS performs the worst. Our proposed MOEA/D-DDS embeds DDS into MOEA/D, which adaptively adjusts the weight vectors at each generation. However, as pointed out in many work [45]-[52], updating the weight vectors too frequently will slow down the convergence speed of the population. Therefore, MOEA/D-DDS may performer worse on MOPs with hardly-convergence PF (like UF10).

Please note that MOEA/D-ACD is developed based on the adaptive *angle-based* constrained decomposition strategy as introduced in **Section 2.2**, while MOEA/D-DDS and NSGA-III apply the *distance-based* constrained decomposition strategy. However, MOEA/D-DDS gives a more promising performance on most UF problems when compared to MOEA/D-ACD and NSGA-III, which strongly demonstrates the superiority of the proposed DDS.

4.3.3 Comparison Results on MOP1-MOP7

MOP1-MOP7 are the widely used benchmark problems, which are modified from ZDT and DTLZ problems. Various twisted search landscapes are embedded into these MOP problems, which pose new challenges to MOEAs, especially on their diversity capability. As the population may be easily trapped into some local regions, it is essential to design a feasible diversity maintenance strategy for balancing the convergence and the diversity in evolution. As explained in [25], both MOEA/D and NSGA-II pay much attentions on promoting the convergence of population, and they have significant difficulties on solving these MOP problems in an efficient way.

Table 7 and **Table 8** respectively list the IGD and HV comparison results of all the seven MOEAs on tackling MOP test problems. When compared to other competitors, MOEA/D-DDS shows the obvious advantages, as it shows significantly better IGD and HV results on all the MOP test problems. The detailed best performance is summarized in the second last row of **Table 7** and **Table 8**. In addition, the Wilcoxon's rank sum test shows the superior performance of MOEA/D-DDS with statistical significance, as summarized in the last row of **Table 7** and **Table 8**.

Overall, the performance of MOEA/D-IR, MOEA/D-ACD and MOEA/D-DDS on MOP test problems overwhelms other competitors. This is mainly because MOEA/D-IR presents an inter-relationship (IR) model to emphasize the diversity, while MOEA/D-ACD and MOEA/D-DDS are designed based on constrained decomposition strategy, which focus on the diversity during the evolutionary search. Although NSGA-III involves the *distance-based* constrained decomposition

Table 7 Performance Comparisons of IGD Values on MOP1-MOP7 Test Problems

Problem	NSGA-III	MOEA/D-DE	MOEA/D-DRA	MOEA/D-STM	MOEA/D-IR	MOEA/D-ACD	MOEA/D-DDS
MOP1	3.65E-01(3.28E-03)–	3.50E-01(3.58E-02)–	3.65E-01(6.10E-03)–	3.62E-01(7.21E-03)–	2.61E-02(2.77E-03)~	2.61E-02(2.60E-03)~	**2.13E-02(1.75E-03)**
MOP2	3.49E-01(1.28E-02)–	2.77E-01(6.70E-02)–	2.43E-01(7.45E-02)–	2.32E-01(6.77E-02)–	3.91E-02(3.35E-02)–	**1.05E-02(1.18E-02)~**	1.21E-02(4.56E-02)
MOP3	9.26E-02(1.04E-02)–	1.07E-01(3.92E-02)–	1.04E-01(5.11E-02)–	1.16E-01(5.51E-02)–	1.23E-02(2.32E-02)–	1.48E-02(2.07E-02)–	**1.20E-02(1.29E-02)**
MOP4	2.96E-01(1.38E-02)–	2.74E-01(2.67E-02)–	2.77E-01(2.59E-02)–	2.81E-01(2.47E-02)–	7.45E-02(8.10E-02)–	7.11E-02(6.11E-02)–	**2.11E-02(2.08E-02)**
MOP5	2.73E-01(2.76E-02)–	3.17E-01(3.70E-03)–	3.16E-01(1.36E-02)–	3.07E-01(5.38E-02)–	2.15E-02(1.74E-03)~	2.33E-02(1.46E-03)–	**1.96E-02(1.90E-03)**
MOP6	3.09E-01(2.51E-05)–	3.02E-01(1.76E-02)–	2.99E-01(2.15E-02)–	3.07E-01(5.63E-03)–	8.51E-02(2.94E-02)–	8.18E-02(2.32E-02)–	**5.00E-02(1.50E-03)**
MOP7	3.56E-01(3.41E-05)–	3.45E-01(2.05E-02)–	3.51E-01(1.39E-02)–	3.54E-01(1.36E-02)–	2.38E-01(3.21E-02)–	3.15E-01(3.15E-02)–	**1.19E-01(4.77E-03)**
Best/All	**0/7**	**0/7**	**0/7**	**0/7**	**0/7**	**1/7**	**6/7**
+/–/~	**0/7/0**	**0/7/0**	**0/7/0**	**0/7/0**	**0/5/2**	**0/5/2**	———

Table 8 Performance Comparisons of HV Values on MOP1-MOP7 Test Problems

Problem	NSGA-III	MOEA/D-DE	MOEA/D-DRA	MOEA/D-STM	MOEA/D-IR	MOEA/D-ACD	MOEA/D-DDS
MOP1	3.077(8.76E-03)–	3.102(6.77E-02)–	3.076(1.40E-02)–	3.080(1.57E-02)–	3.623(3.10E-02)–	3.629(3.24E-03)~	**3.630(2.90E-03)**
MOP2	3.003(7.23E-03)–	3.038(4.06E-02)–	3.062(6.37E-02)–	3.079(5.57E-02)–	3.174(1.10E-01)–	3.287(1.03E-01)–	**3.304(4.80E-02)**
MOP3	3.105(1.17E-02)–	3.081(4.03E-02)–	3.087(5.60E-02)–	3.073(6.13E-02)–	3.184(5.25E-02)–	2.961(2.74E-01)–	**3.197(2.06E-02)**
MOP4	3.135(9.62E-03)–	3.151(2.32E-02)–	3.151(2.35E-02)–	3.148(2.23E-02)–	3.044(2.46E-01)–	3.019(1.56E-01)–	**3.484(3.04E-02)**
MOP5	3.116(1.10E-01)–	2.723(1.16E-01)–	2.711(1.11E-01)–	2.755(2.08E-01)–	3.632(4.37E-03)~	3.626(3.77E-03)–	**3.633(2.86E-03)**
MOP6	7.495(4.23E-04)–	7.502(2.63E-02)–	7.508(3.20E-02)–	7.497(8.50E-03)–	7.732(3.07E-02)–	7.730(1.94E-02)–	**7.766(2.73E-03)**
MOP7	7.209(6.08E-04)–	7.213(1.16E-02)–	7.210(4.43E-03)–	7.212(7.76E-03)–	7.288(4.74E-02)–	7.195(3.13E-02)–	**7.350(3.46E-03)**
Best/All	**0/7**	**0/7**	**0/7**	**0/7**	**0/7**	**0/7**	**7/7**
+/–/~	**0/7/0**	**0/7/0**	**0/7/0**	**0/7/0**	**0/6/1**	**0/6/1**	———

strategy, it is also easily trapped into some local regions on these problems due to its niche-preservation method to emphasize the convergence first. Moreover, as DDS is further used to reproduce the suitable weight vectors for the constrained decomposition strategy, MOEA/D-DDS performs significantly better than MOEA/D-ACD on both IGD and HV. Therefore, the effectiveness of the proposed DDS is validated, which is the main difference between MOEA/D-DDS and MOEA/D-ACD.

4.4 Further Discussion and Analysis on MOEA/D-DDS

To quantify how well each algorithm performs overall with a more vigorous multi-method statistical test, Friedman's test is used to rank these compared algorithms on all the test problems. Please note that the software tool KEEL [67] is used here to conduct Friedman's test. In **Fig. 6**, the average performance rank is summarized for different test problems, and the ranks of MOEA/D-DDS are connected by a red line to easily observe the values. The ranks on all the problems shows the average performance rank of the selected seven MOEAs when solving all the twenty-six test problems. A smaller performance rank indicates a better performance for this algorithm.

From the IGD based average rankings in **Fig. 6(a)**, MOEA/D-DDS has the best rank on all the test problems adopted. Regarding WFG1-WFG9 and UF1-UF10, MOEA/D-DDS obtains the second and third ranks, respectively. From the HV based average rankings in **Fig. 6(b)**, MOEA/D-DDS gives the second rank on UF1-UF10 and WFG1-WFG9. Especially, MOEA/D-ACD has a better rank on

MOP1-MOP7, but a worse rank on other test problems; NSGA-III has a better rank on WFG1-WFG9, but performs worse on other test problems. Thus, the ranks in **Fig. 6** clearly illustrate the comprehensive performance of MOEA/D-DDS on all test problems.

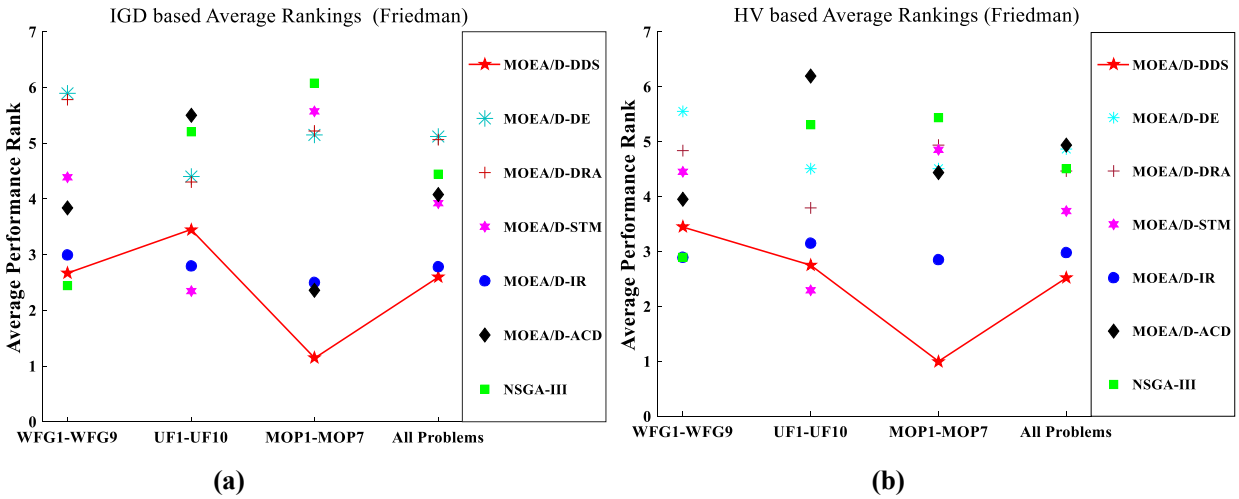

(a) **(b)**

Fig. 6 Average performance ranks of the selected seven MOEAs on different test problems with Friedman's test

To visually show and support the above discussion results, some final solution sets with the median IGD values from 30 runs are plotted in **Figs. 7-12**, respective for UF1 with an regular PF, UF9 with complicated two disconnected PFs, MOP1 with a simple twisted search landscapes and a regular PF, MOP4 with a disconnected PF and a twisted search landscapes, MOP6 with three-objective PF, and WFG9 with a different scaled PF. It is also used for a better understanding on the performance of seven MOEAs and to describe the distribution of obtained solutions in the objective space.

Regarding UF1, UF2, and UF7 with the similar PFs, UF1 is shown in **Fig. 7** as an example. Obviously, only NSGA-III has difficulty in solving UF1, as the obtained set of optimum solutions is not so smooth and unable to approximate the true PF, while MOEA/D-DE, MOEA/D-DRA, MOEA/D-STM, MOEA/D-IR, MOEA/D-ACD and MOEA/D-DDS all perform well in approximating the entire PF of UF1, which have the similar distributions of solutions. For the three-objective problem UF9 shown in **Fig. 8**, when comprehensively considering the convergence and diversity of the obtained solution sets of these seven MOEAs, MOEA/D-DDS, MOEA/D-IR and MOEA/D-STM are almost able to approximate the two disconnected PFs of UF9, while NSGA-III only converges to the topmost segment and MOEA/D-ACD only converges to the rightmost segment. For MOEA/D-DE and MOEA/D-DRA, the distributions of solutions are not so smooth and a couple of regions along the true PF are lost. For MOP test problems (MOP1, MOP4 and MOP6) shown in **Figs. 9-11**, it is clear that only MOEA/D-DDS, MOEA/D-IR and MOEA/D-ACD can approximate the entire true PF, while other MOEAs are all falling into a couple of local regions along the true PF. In special, for MOP1 in **Fig. 9**,

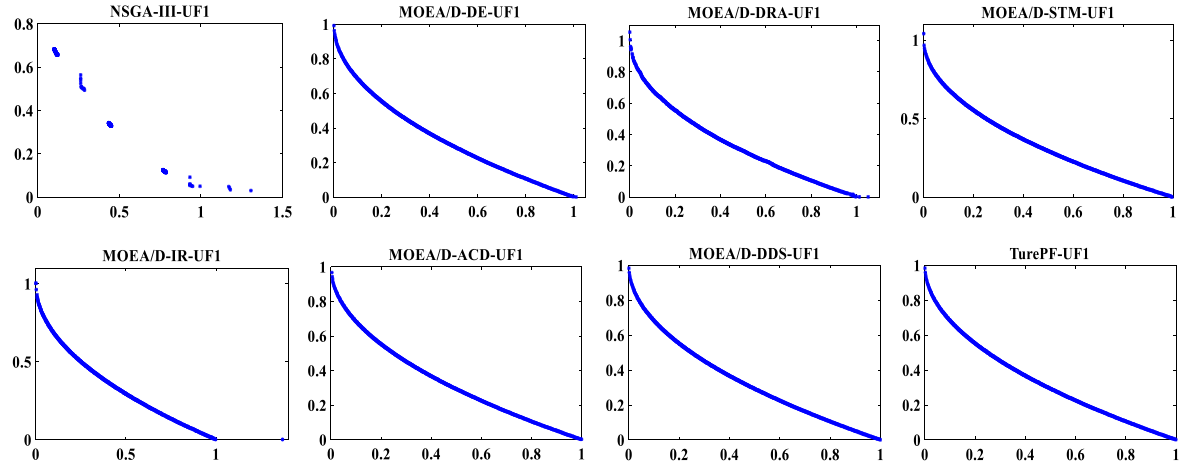

Fig. 7 Final solution sets achieved by seven MOEAs and the true PF on UF1 problems

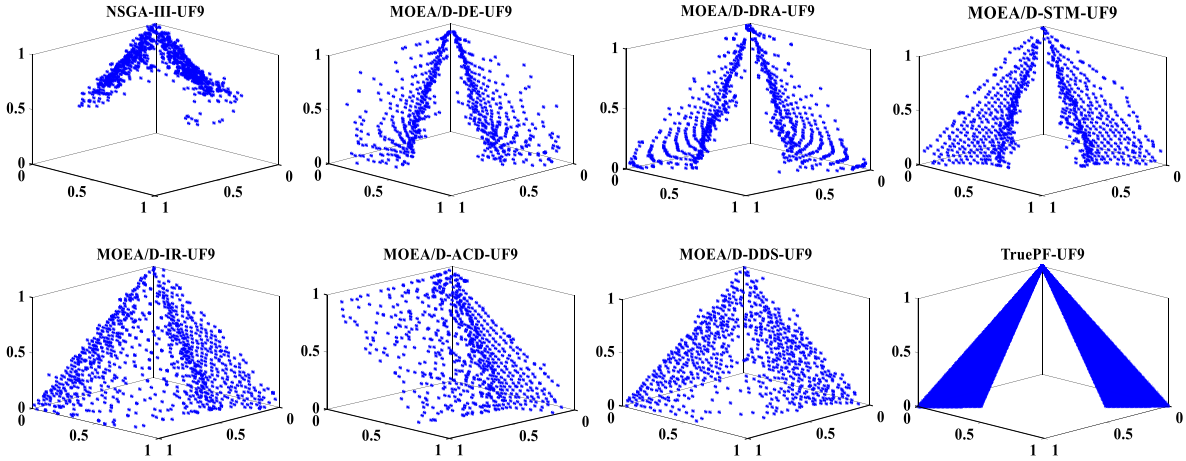

Fig. 8 Final solution sets achieved by seven MOEAs and the true PF on UF9 problems

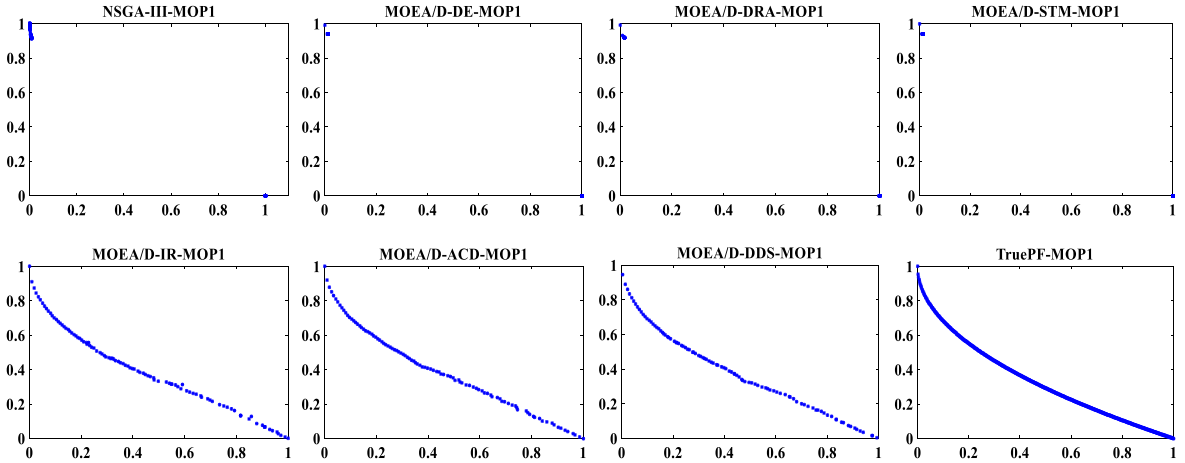

Fig. 9 Final solution sets achieved by seven MOEAs and the true PF on MOP1 problems

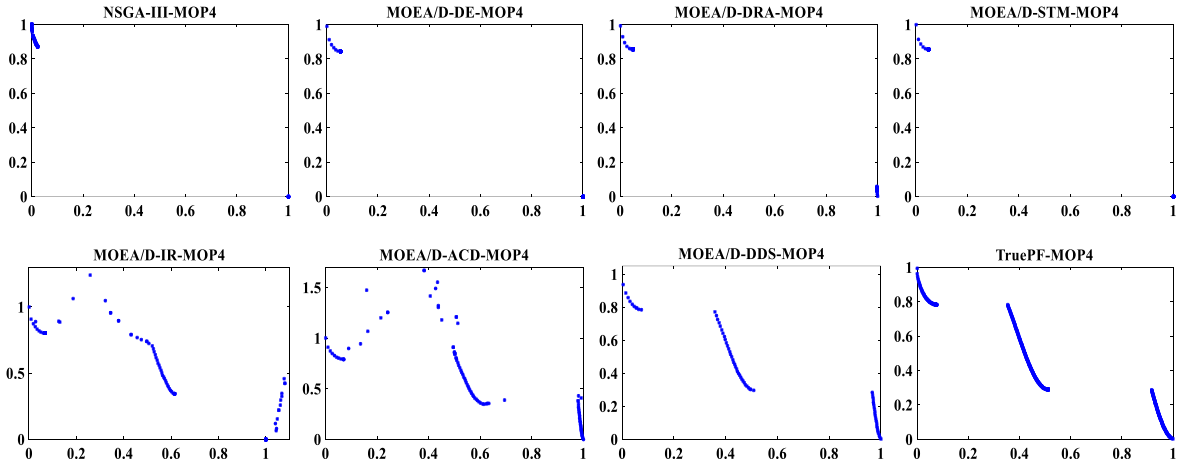

Fig. 10 Final solution sets achieved by seven MOEAs and the true PF on MOP4 problems

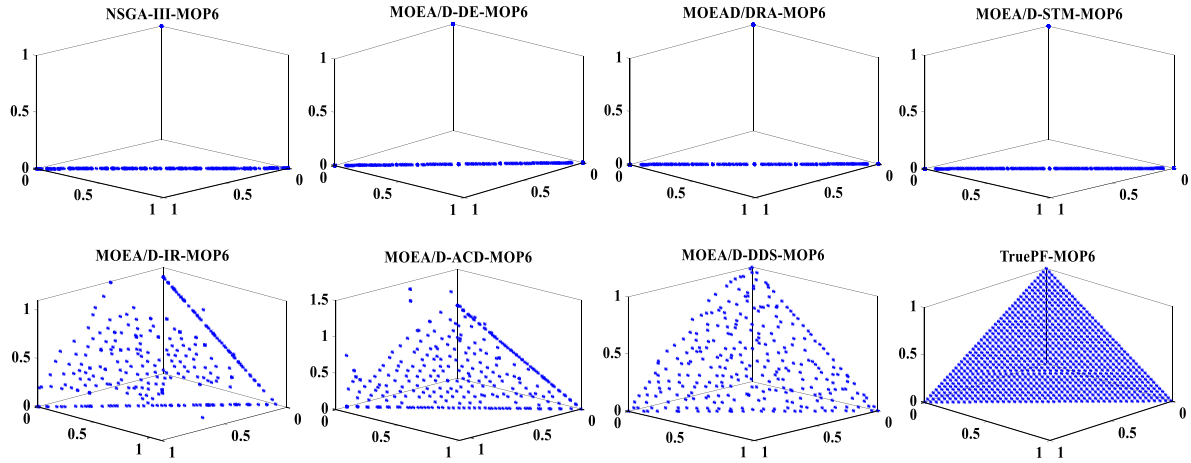

Fig. 11 Final solution sets achieved by seven MOEAs and the true PF on MOP6 problems

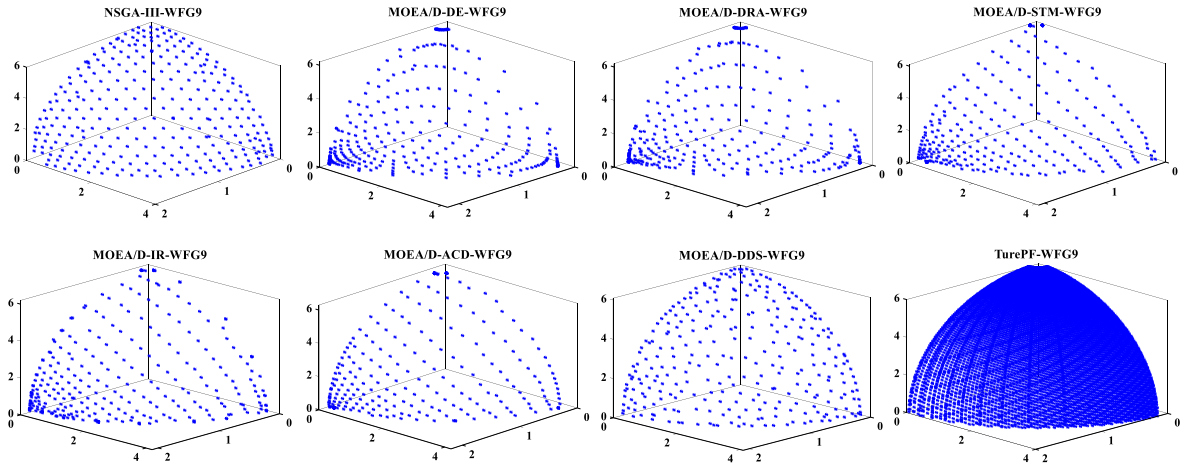

Fig. 12 Final solution sets achieved by seven MOEAs and the true PF on WFG9 problems

the solutions obtained by MOEA/D-DDS are smoother than those of MOEA/D-IR and MOEA/D-ACD. On MOP4 consisting of three disconnected segments in **Fig. 10**, MOEA/D-DDS and MOEA/D-ACD can well approximate the middle and rightmost segments of the true PF, while solutions obtained by MOEA/D-IR mainly cover the middle and leftmost segments of the true PF. Regarding MOP6 in **Fig. 11** which has a regular three-objective true PF developed from DTLZ1, MOEA/D-DDS has a better spread over the true PF than MOEA/D-IR and MOEA/D-ACD. With respect to WFG9 in Fig. 12, its PF has a different scale in each objective, and NSGA-III performs very well as the used weight vectors can well match the PF after the normalization process. Other compared MOEA/D variants also give the promising performance and MOEA/D-DDS seems to have a better distribution. Thus, these figures fully validate the results discussed in **Section 4.3** and illustrate the superiority of MOEA/D-DDS in solving MOPs with irregular and regular PFs.

Table 9 *p*-values Obtained by Four Post Hoc Procedure for The Compared MOEAs

MOEA/D-DDS	vs.	*p-unadjusted*	*p-Bonf*	*p-Holm*	*p-Hoch*	*p-Homm*
On All Problems (HV)	MOEA/D-ACD	**0.000052**	**0.000315**	**0.000315**	**0.000315**	**0.000270**
	MOEA/D-DE	**0.000090**	**0.000541**	**0.000450**	**0.000450**	**0.000450**
	NSGA-III	**0.000946**	**0.005678**	**0.003786**	**0.003563**	**0.002839**
	MOEA/D-DRA	**0.001188**	**0.007127**	**0.003786**	**0.003563**	**0.003563**
	MOEA/D-STM	0.043165	0.258988	0.086329	0.086329	0.086329
	MOEA/D-IR	0.441105	2.646629	0.441105	0.441105	0.441105
MOEA/D-DDS	vs.	*p-unadjusted*	*p-Bonf*	*p-Holm*	*p-Hoch*	*p-Homm*
On MOP Problems (HV)	NSGA-III	**0.000125**	**0.000753**	**0.000753**	**0.000753**	**0.000753**
	MOEA/D-DRA	**0.000668**	**0.004010**	**0.003342**	**0.003342**	**0.002673**
	MOEA/D-STM	**0.000837**	**0.005020**	**0.003347**	**0.003347**	**0.003347**
	MOEA/D-DE	**0.002437**	**0.014620**	**0.007310**	**0.005971**	**0.004873**
	MOEA/D-ACD	**0.002985**	**0.017913**	**0.007310**	**0.005971**	**0.005971**
	MOEA/D-IR	0.107762	0.646574	0.107762	0.107762	0.107762
MOEA/D-STM	vs.	*p-unadjusted*	*p-Bonf*	*p-Holm*	*p-Hoch*	*p-Homm*
On UF Problems (HV)	MOEA/D-ACD	0.000054	0.000325	0.000325	0.000325	0.000325
	NSGA-III	0.001901	0.011405	0.009504	0.009504	0.009504
	MOEA/D-DE	0.022773	0.136640	0.091093	0.091093	0.091093
	MOEA/D-DRA	0.120507	0.723044	0.361522	0.361522	0.361522
	MOEA/D-IR	0.378949	2.273697	0.757899	0.641363	0.641363
	MOEA/D-DDS	0.641363	3.848177	0.757899	0.641363	0.641363
NSGA-III	vs.	*p-unadjusted*	*p-Bonf*	*p-Holm*	*p-Hoch*	*p-Homm*
On WFG Problems (HV)	MOEA/D-DE	0.008829	0.052973	0.052973	0.052973	0.052973
	MOEA/D-DRA	0.056210	0.337258	0.281048	0.281048	0.281048
	MOEA/D-STM	0.126630	0.759783	0.506522	0.506522	0.506522
	MOEA/D-ACD	0.299953	1.799716	0.899858	0.899858	0.878068
	MOEA/D-DDS	0.585379	3.512274	1.170758	1.000000	1.000000
	MOEA/D-IR	1.000000	6.000000	1.170758	1.000000	1.000000

In addition, to further test the significant difference among these compared algorithms, the *p*-values obtained by Bonferroni-Dunn's, Holm's, Hochberg's and Hommel's post hoc procedure using the software tool KEEL [67] are listed in **Table 9**. These *p*-values are all obtained based on the HV results of each MOEA on different test problems, which indicate that the comprehensive performance of MOEA/D-DDS is significantly better than other compared MOEAs on all the test problems adopted.

As shown in **Table 9**, although the comprehensive performance of MOEA/D-DDS is worse than that of MOEAD-STM on the UF test problems and worse than that of NSGA-III and MOEA/D-IR on the WFG test problems, the comparison results between them are very similar as observed from the relatively large *p*-values in these post hoc procedures. Other *p*-values are very closer to 0, which indicate the significant differences on the experimental results.

In summary, among the six compared MOEAs, it is reasonable to conclude that MOEA/D-DDS is the best one on tackling most of test MOPs adopted, which is largely brought by the proposed DDS. In our proposed DDS, the diversity and convergence of the population are considered simultaneously by dynamically generating the weight vectors based on the distribution of the population.

4.5 More discussions about DDS

As discussed in **Section 3.3**, our designed DDS includes three main components, i.e., *distance-based* constrained decomposition approach (Eq. (5)), clustering-based dynamic decomposition (**Algorithm 3**) and the convergence-based solution selection method (Eq. (14)). After observing the above extensive experimental results, it is found that the approach in **Algorithm 3** has the greatest impact on the results of MOEA/D-DDS when compared to other two components of DDS. Here, the approach of Eq. (5) can be replaced with *angle-based* approach defined in Eq. (4) and several alternative convergence indicators (such as the Euclidean distance to the ideal point and also to the Nadir point) can be applied into DDS to achieve the similar performance on most of test MOPs used. For **Algorithm 3**, there are two main factors to be considered, i.e., the selection of clustering method and the selection of subproblems to be decomposed.

Based on the existing experimental studies, the agglomerative hierarchical clustering method is the most reasonable one for DDS in solving various MOPs, as it not only obtains the best performance, but also has the suitable computational complexity for DDS. Moreover, when considering the selection of subproblem to be decomposed, it is a straightforward ideal to decompose the subproblem with the highest density in its feasible region, as introduced in **Section 3.3**. Of course, there are other strategies that can be considered. As shown in **Fig. 13(a)**, the feasible region of 2^{rd} subproblem has the largest number of associated solutions, thus the 2^{rd} subproblem needs to be decomposed by **Algorithm 3** based on the introduced DDS in **Section 3.3**. However, while doing this procedure, some information about 3^{th} and 4^{th} sub-regions may be lost due to an overweight exploration in 2^{rd} sub-region. In this case, we can also consider to select other subproblem to be decomposed. Here, another strategy is to select the sub-region with the maximum span, in which the definition of a region's maximum span can be defined by the maximum angle between any two solutions in this region (if only one or no solution is within this region, the maximum span is set to 0). Therefore, using this selection strategy, **Algorithm 3** is run on the 3^{th} subproblem as shown in **Fig. 13(b)**.

In order to show the efficiency of the above alternative strategy for selecting the subproblem to be decomposed, some experimental studies are given with the same parameter settings in **Table 2**. In this experiment, case1 indicates MOEA/D-DDS using the strategy of selecting the subproblem with the highest density to be decomposed in **Algorithm 3**, while case2 means an alternative strategy to decompose the subproblem with the maximum span. **Table 10** gives a summary of the significance test on the HV and IGD comparison results obtained by case1 and case2 of MOEA/D-DDS, when tackling twenty-six test problems. It can be observed from **Table 10** that a lot of similar performance are obtained by case1 and case2, as there are 11 similar ones out of total 26 cases on both IGD and HV, while case1 performs slightly better than case2 when considering all the test problems. In special, as shown in **Fig. 14**, case2 performs better than case1 in exploring the boundary region of UF8, which indicates the efficiency of case2 in MOEA/D-DDS to tackle some kinds of MOPs.

Overall, there are many factors to influence the performance of our proposed DDS, and the DDS introduced in **Section 3.3** is more reasonable for MOEA/D-DDS to solve most of test MOPs adopted in this paper.

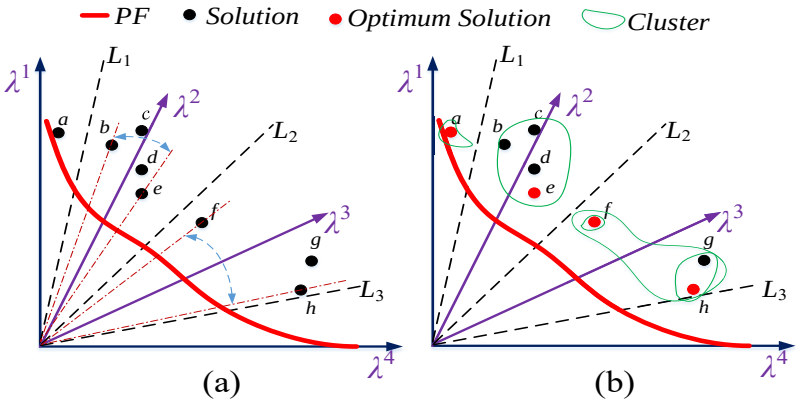

Fig. 13 A simple example to show the process of case2 in MOEA/D-DDS

Table 10 Summary of the Significance Test between case1 and case2 of MOEA/D-DDS

case1	vs	case2	case 1	vs	case2
With IGD metric	Better	8	With HV metric	Better	9
	Worse	7		Worse	6
	Similar	11		Similar	11

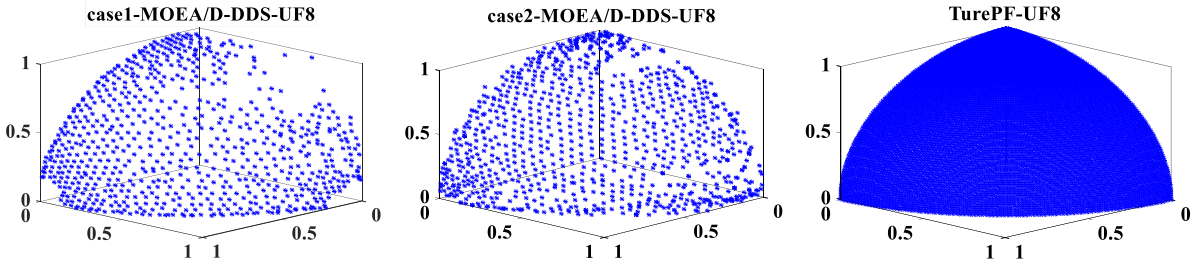

Fig. 14 The final solution sets achieved by MOEA/D-DDS with case1 and case2

4.6 More studies on the Comparison of MOEA/D-DDS

In the previous subsections (**Section 4.3.1** to **Section 4.3.3**), we have experimentally verified the advantages of our proposed MOEA/D-DDS in solving different kinds of MOPs (WFG, UF and MOP) when compared to some competitive decomposition-based MOEAs. To further verify the advantages of MOEA/D-DDS over other kinds of MOEAs, like dominance-based and indicator-based MOEAs, more experimental studies are conducted in this section. Moreover, in order to further verify the effectiveness and efficiency of DDS, a recent decomposition-based MOEAs with a learning-to-decompose paradigm (MOEA/D-LTD [72]) is also compared. At last, we also study the performance of MOEA/D-DDS on solving some many-objective optimization problems (MaOPs) that the number of objective m is more than three (m>3).

4.6.1 Comparison results with other kinds of MOEA

Here, two dominance-based MOEAs (ε-MOEA[68] and VaEA [69]), two indicator-based MOEAs (MOEA/IGD-NS [70] and SMS-EMOA [71]), a MOEA based on the bi-criterion evolution framework of dominance-based criterion and indicator-based criterion (BEC-IBEA [19]), and MOEA/D-LTD [72] were included for performance comparison. To allow a fair comparison, the related parameters of all the compared algorithms were set as suggested in their references. Besides, seventeen test problems (UF1-UF10 and MOP1-MOP7) were adopted, and all the parameter settings of these test problems were set the same as introduced in **Section 4. 1**. Finally, the IGD metric introduced in Section 4.1.3 was used as the performance indicator.

Table 11 Performance Comparisons of IGD values on UF1-UF10 and MOP1-MOP7

Problem	ε-MOEA	BCE-IBEA	MOEA/IGD-NS	SMS-EMOA	VaEA	MOEA/D-LTD	MOEA/D-DDS
UF1	1.22E-01(3.36E-02)	4.07E-02(8.01E-04)	8.69E-02 (5.11E-04)	7.41E-02(1.04E-04)	9.93E-02(6.65E-03)	5.09E-02(1.11E-02)	**1.03E-03(7.81E-05)**
UF2	6.32E-02(9.90E-03)	3.40E-02(6.07E-03)	3.16E-02(4.13E-03)	5.48E-02(5.62E-03)	2.92E-02(1.75E-03)	1.35E-02(3.66E-03)	**5.63E-03(1.35E-03)**
UF3	1.49E-01(4.59E-02)	5.65E-02(5.05E-02)	5.07E-02(3.19E-02)	5.28E-02(4.77E-02)	6.99E-02(4.33E-02)	7.55E-02(6.14E-02)	**7.90E-03(2.74E-03)**
UF4	7.42E-02(3.02E-03)	4.07E-02(1.52E-03)	4.29E-02(3.60E-03)	4.17E-02(2.91E-03)	4.16E-02(9.09E-04)	**3.36E-02(1.15E-03)**	5.28E-02(2.99E-03)
UF5	2.56E-01(5.39E-02)	**1.96E-01(2.94E-02)**	2.08E-01(4.23E-02)	2.26E-01(2.22E-02)	2.19E-01(4.50E-02)	2.25E-01(7.95E-02)	2.70E-01(2.10E-02)
UF6	2.07E-01(1.08E-01)	2.13E-01(1.85E-01)	2.10E-01(1.83E-01)	2.16E-01(1.67E-01)	1.23E-01(8.47E-02)	1.61E-01(1.21E-01)	**7.38E-02(2.32E-02)**
UF7	2.27E-01(1.41E-02)	2.00E-02(1.04E-02)	4.57E-02(1.11E-02)	4.81E-02(2.00E-02)	3.21E-02(7.01E-03)	1.09E-01(1.30E-02)	**3.58E-03(9.21E-04)**
UF8	4.97E-01(8.62E-02)	2.07E-01(3.02E-02)	3.25E-01(4.21E-02)	3.84E-01(5.27E-02)	2.34E-01(6.19E-03)	8.22E-02(7.09E-03)	**5.21E-02(8.24E-03)**
UF9	3.76E-01(4.70E-02)	1.52E-01(3.09E-02)	3.90E-01(5.99E-02)	4.91E-01(8.78E-02)	2.43E-01(3.49E-02)	7.88E-02(2.82E-02)	**2.66E-02(5.70E-03)**
UF10	5.10E-01(6.37E-02)	1.56E+0(2.73E-01)	3.47E-01(2.16E-02)	3.75E-01(4.00E-02)	2.98E-01(5.71E-02)	**2.08E-01(2.11E-02)**	1.75E+00(2.53E-01)
MOP1	3.84E-01(8.44E-03)	3.14E-01(8.12E-03)	3.40E-01(8.37E-03)	3.01E-01(7.46E-03)	3.42E-01(8.65E-03)	6.15E-02(5.55E-03)	**2.13E-02(1.75E-03)**
MOP2	3.54E-01(7.78E-02)	2.10E-01(5.18E-02)	2.20E-01(6.61E-02)	2.09E-01(6.04E-02)	3.54E-01(8.11E-02)	1.11E-01(2.38E-02)	**1.21E-02(4.56E-02)**
MOP3	5.78E-01(4.20E-02)	1.10E-01(4.60E-02)	1.13E-01(9.16E-02)	1.10E-01(2.03E-02)	5.06E-01(8.39E-02)	1.51E-01(7.11E-02)	**1.20E-02(1.29E-02)**
MOP4	3.45E-01(1.83E-02)	3.51E-01(3.23E-02)	3.38E-01(3.31E-02)	3.53E-01(1.83E-02)	3.06E-01(1.35E-02)	1.45E-01(8.15E-02)	**2.11E-02(2.08E-02)**
MOP5	3.15E-01(4.08E-03)	4.84E-01(5.41E-02)	5.34E-01(4.06E-02)	4.84E-01(6.16E-02)	2.67E-01(3.64E-02)	5.35E-02(7.08E-03)	**1.96E-02(1.90E-03)**
MOP6	3.11E-01(1.05E-03)	8.29E-01(4.77E-03)	8.28E-01(4.91E-03)	8.21E-01(4.35E-03)	3.09E-01(8.94E-03)	8.44E-02(8.26E-03)	**5.00E-02(1.50E-03)**
MOP7	3.64E-01(3.30E-03)	5.44E-01(7.33E-03)	5.43E-01(7.81E-03)	5.35E-01(6.30E-03)	3.57E-01(5.13E-03)	**1.06E-01(5.14E-03)**	1.19E-01(4.77E-03)
Best/All	**0/17**	**1/17**	**0/17**	**0/17**	**0/17**	**3/17**	**13/17**

The mean IGD results of these seven MOEAs on UF1-UF10 and MOP1-MOP7 are reported in Table 11. It can be observed that MOEA/D-DDS obtains significantly better results for 13 out of 17 test problems, while ε-MOEA, BEC-IBEA, MOEA/IGD-NS, SMS-EMOA, VaEA and MOEA/D-LTD are best on 0, 1, 0, 0, 0 and 3, respectively. Therefore, MOEA/D-DDS shows superior performance on most

of UF and MOP problems when compared to these MOEAs, which also demonstrates the superiority of the proposed DDS.

4.6.2 Comparison results on test problems with 5 and 10 objectives

Recently, decomposition-based MOEAs have showed their effectiveness and efficiency when solving MaOPs. However, it was experimentally studied and pointed out in [47] that the performance of decomposition-based MOEAs strongly depends on the consistency to the shapes of the PF and the used weight vectors. As the weight vectors of MOEA/D-DDS are adaptively generated by DDS, MOEA/D-DDS can be directly applied to solve MaOPs in this part. In order to testify the performance of DDS in tackling MaOPs, four recently proposed many-objective evolutionary algorithms (MaOEAs) were used for comparison, i.e., NSGA-III [55], θ-DEA [66], EFR-RR [73] and VaEA [69]. In addition, MaF1, MaF2 and MaF7 from an irregular and complex MaOP series: MaF [74], and WFG1-WFG4 and WFG9 were used for experimental studies. For each problem, the number of objectives m was set to 5 and 10. Correspondingly, the population size N is set to 210 and 275 for 5- and 10-objective problems, respectively. Moreover, the number of decision variables n in MaF series was set by n=m+k-1, where k was set to 10 for MaF1-MaF2 and to 20 for MaF7. Regarding the WFG problems, k (position-related parameters) was set to 2(m-1) and l (distance-related parameters) was set to 20. All the algorithms were terminated when a predefined maximum number of generations G_{max} was reached. The values of G_{max} for 5- and 10-objective problems were set to 600 and 900, respectively. Moreover, the normalized HV metric was used as the performance indicator, where the objective vectors in final solution sets were all normalized by $1.1\times(f_1^{\max}, f_2^{\max},..., f_m^{\max})$, where $f_k^{\max}$ (k = $1,2,...,m$) was the maximum value of kth objective in the true PF, and then the reference point was set to $(1.0,1.0,...,1.0)$.

Table 12 Performance comparisons of normalized HV values on 5- and 10-objective Problems

Problem	Obj. (m)	NSGA-III	θ-DEA	EFR-RR	VaEA	MOEA/D-DDS
MaF1	m=5	6.419E-03(6.10E-04)–	4.129E-03(3.25E-04)–	2.355E-03(4.91E-04)–	1.081E-02(7.36E-04)–	**7.519E-03(1.63E-04)**
	m=10	3.824E-07(5.54E-08)–	2.583E-07(6.17E-08)–	1.400E-07(8.31E-08)–	2.314E-07(4.54E-08)–	**4.378E-07(2.79E-08)**
MaF2	m=5	2.368E-01(2.26E-03)–	2.275E-01(3.42E-03)–	2.122E-01(3.14E-03)–	2.247E-01(3.52E-03)–	**2.445E-01(3.88E-03)**
	m=10	2.023E-01(3.96E-03)–	1.841E-01(7.62E-03)–	1.853E-01(4.18E-03)–	1.992E-01(6.24E-03)~	**2.097E-01(3.25E-03)**
MaF7	m=5	2.966E-01(2.18E-03)~	2.680E-01(7.09E-03)–	1.996E-01(2.82E-02)–	2.985E-01(2.58E-03)~	**3.061E-01(2.12E-03)**
	m=10	2.267E-01(3.01E-03)–	2.205E-01(1.63E-02)–	1.290E-01(1.52E-02)–	1.833E-01(8.84E-03)–	**2.359E-01(3.14E-03)**
WFG1	m=5	3.524E-01(2.96E-02)–	5.221E-01(2.72E-02)–	3.432E-01(2.04E-02)–	3.135E-01(3.21E-02)–	**5.410E-01(2.19E-02)**
	m=10	6.438E-01(4.01E-02)–	**8.634E-01(9.43E-03)+**	7.537E-01(3.39E-02)+	7.009E-01(3.14E-02)+	6.649E-01(5.71E-02)
WFG2	m=5	9.490E-01(5.23E-02)+	9.435E-01(6.54E-02)+	**9.799E-01(2.36E-03)+**	9.586E-01(3.11E-02)+	9.351E-01(4.69E-02)
	m=10	9.501E-01(5.99E-02)–	9.003E-01(8.50E-02)–	9.616E-01(5.82E-02)~	**9.783E-01(3.39E-03)+**	9.620E-01(8.90E-03)
WFG3	m=5	6.104E-01(7.72E-03)+	**6.298E-01(7.32E-03)+**	5.803E-01(8.18E-03)~	5.594E-01(1.34E-02)–	5.839E-01(9.61E-03)
	m=10	**6.196E-01(2.75E-02)+**	6.003E-01(1.97E-02)~	6.011E-01(1.55E-02)~	5.283E-01(3.53E-02)–	6.002E-01(2.44E-02)
WFG4	m=5	7.111E-01(6.46E-03)+	**7.425E-01(4.61E-03)+**	7.269E-01(5.01E-03)+	7.007E-01(6.37E-03)~	7.066E-01(3.13E-03)
	m=10	8.511E-01(9.95E-03)+	**8.642E-01(9.14E-03)+**	8.478E-01(1.16E-02)+	8.125E-01(1.00E-02)–	8.459E-01(7.17E-03)
WFG9	m=5	6.533E-01(1.48E-02)–	6.921E-01(1.77E-02)~	6.416E-01(7.99E-03)–	6.376E-01(5.36E-03)–	**6.713E-01(3.25E-03)**
	m=10	7.229E-01(1.23E-02)–	7.490E-01(2.67E-02)~	7.292E-01(2.41E-02)–	6.979E-01(1.20E-02)–	**7.508E-01(1.03E-02)**
Best/All		**1/16**	**4/16**	**1/16**	**1/16**	**9/16**
+/–/~		**5/1/10**	**5/3/8**	**4/3/9**	**3/3/10**	———

Table 12 provides the mean HV comparison results of MOEA/D-DDS with respect to four current MaOEAs (NSGA-III, θ-DEA, EFR-RR and VaEA) on MaF1, MaF2, MaF7, WFG1-WFG4 and WFG9 with 5 and 10 objectives. As observed from Table 12, MOEA/D-DDS obtains the best results on 9 out of 16 comparisons, which validates the superior performance of MOEA/D-DDS on solving MaOPs, especially for the irregular problems like MaF1 with an inverted PF and MaF7 with a disconnected PF. For NSGA-III, θ-DEA, EFR-RR and VaEA, they respectively obtain the best results on 1, 4, 1 and 1 out of 16 comparisons. As observed from the one-to-one comparisons in the last row of Table 12, MOEA/D-DDS respectively performs better than NSGA-III, θ-DEA, EFR-RR and VaEA on 10, 8, 9 and 10 out of 16 comparisons; whereas, MOEA/D-DDS is only beaten by NSGA-III, θ-DEA, EFR-RR and VaEA on 5, 5, 4 and 3 comparisons, respectively. Therefore, MOEA/D-DDS also shows a superior performance on solving MaOPs when compared to these four MaOEAs, which further justifies the advantages of the proposed DDS.

5. Conclusions and future work

In this paper, a novel decomposition-based MOEA with dynamic decomposition strategy was presented, named MOEA/D-DDS. This approach firstly decomposes a MOP in Eq. (1) into a set of constrained subproblems by using a set of uniformly distributed weight vectors. Then, based on the proposed DDS, one most crowded feasible region is found and decomposed into two new subproblems in the objective space. This process of dynamic decomposition will be run a number of times until there have N subproblems, and each one is associated with at least one solution. At last, one individual showing the best convergence is selected from each of N subproblems to form the new population for next generation. Under this way, MOEA/D-DDS can well balance diversity and convergence by considering the distribution of evolutionary population. When compared to six decomposition-based MOEAs (NSGA-III, MOEA/D-DE, MOEA/D-DRA, MOEA/D-STM, MOEA/D-IR, and MOEA/D-ACD) and other kinds of MOEAs (ε-MOEA, VaEA, MOEA/IGD-NS, SMS-EMOA, MOEA/D-LTD), MOEA/D-DDS showed some advantages on tackling most of the test problems adopted.

In our future work, we will further study other decomposition approaches using the machining learning methods. Moreover, the application of MOEA/D-DDS to solve the real-life problems will be conducted as part of our future work.

Acknowledge

This work was supported by the National Natural Science Foundation of China under Grants 61876110, 61803269, 61836005, and 61672358, the Joint Funds of the National Natural Science Foundation of China under Key Program Grant U1713212, the Natural Science Foundation of Guangdong Province under Grant 2017A030313338, the Fundamental Research Project in the Science and Technology Plan of Shenzhen under Grants JCYJ20170817102218122 and

JCYJ20170302154032530, and CONACyT Grant no. 221551. Also, this work was supported by the National Engineering Laboratory for Big Data System Computing Technology.

References

[1] S.S. Jimenez and M.A.V. Rodriguez, Performance evaluation of dominance-based and indicator-based multiobjective approaches for phylogenetic inference, Information Sciences, 330 (2016) 293–314.

[2] P. Shelokar, A. Quirin, O. Cordon, A multiobjective evolutionary programming framework for graph-based data mining, Information Sciences, 237 (2013) 118–136.

[3] P. Ekel, I. Kokshenev, R. Parreiras, W. Pedrycz, J.P. Jr, Multiobjective and multiattribute decision making in a fuzzy environment and their power engineering applications, Information Sciences, 361-362 (2016) 100–119.

[4] A. Rubio-Largo, Q. Zhang, M.A. Vega-Rodriguez, A multiobjective evolutionary algorithm based on decomposition with normal boundary intersection for traffic grooming in optical networks, Information Sciences, 289 (2014) 91–116.

[5] A. Ponsich, A.L. Jaimes, and C.A.C. Coello, A survey on multiobjective evolutionary algorithms for the solution of the portfolio optimization problem and other finance and economics applications, IEEE Trans. Evol. Comput., 17(3) (2013) 321–344.

[6] A. Ropponen, R. Ritala, and E.N. Pistikopoulos, Optimization issues of the broke management system in papermaking, Comput. Chem. Eng., 35(11) (2011) 2510–2520.

[7] K. Miettinen, *Nonlinear Multiobjective Optimization*, Boston, Ma, USA: Kluwer Academic, 1999

[8] K. Deb, Multi-Objective Optimization Using Evolutionary Algorithms, Chichester, U.K.: Wiley, 2001.

[9] A. Zhou et al., Multiobjective evolutionary algorithms: A survey of the state of the art, Swarm Evol. Comput., 1(1) (2011) 32–49.

[10] C.A.C. Coello, Evolutionary multi-objective optimization: A historical view of the field, IEEE Comput. Intell. Mag., 1(1) (2006) 28–36.

[11] K. Deb, A. Pratap, S. Agarwal, and T. Meyarivan, A fast and elitist multiobjective genetic algorithm: NSGA-II, IEEE Trans. Evol. Comput., 6(2) (2002) 182–197.

[12] E. Zitzler, M. Laumanns, and L. Thiele, SPEA2: Improving the strength Pareto evolutionary algorithm for multiobjective optimization, in Proc. Evol. Methods Des., Optimisation Control., (2002) 95–100.

[13] T. Pamulapati, R. Mallipeddi, P. N. Suganthan, ISDE+-An Indicator for Multi and Many-objective Optimization, in press, doi: 10.1109/TEVC.2018.2848921, 2018.

[14] J. Bader and E. Zitzler, HypE: an algorithm for fast hypervolume based many-objective optimization, Evolutionary Computation, 19(1) (2011) 45–76.

[15] Q.F. Zhang and H. Li, MOEA/D: A multiobjective evolutionary algorithm based on decomposition, IEEE Trans. Evol. Comput., 11(6) (2007) 712–731.

[16] S. Zhao, P. N. Suganthan, Q. Zhang, Decomposition-Based Multiobjective Evolutionary Algorithm with an Ensemble of Neighborhood Sizes, IEEE Trans. Evol. Comput., 16(3) (2012) 442-446.

[17] E. Zitzler and L. Thiele, Multiobjective evolutionary algorithms: A comparative case study and the strength Pareto approach, IEEE Trans. Evol. Comput., 3(4) (1999) 257–271.

[18] H. Ishibuchi, N. Akedo, and Y. Nojima, Behavior of multiobjective evolutionary algorithms on many-objective

Knapsack problems, IEEE Trans. Evol. Comput., 19(2) (2015) 264–283.

[19] M. Li, S. Yang, and X. Liu, Pareto or non-pareto: Bi-criterion evolution in multiobjective optimization, IEEE Trans. Evol. Comput., 20(5) (2016) 645–665.

[20] H. Sato, Chain-reaction solution update in MOEA/D and its effects on multi- and many-objective optimization, Soft Comput, 20 (2016) 3803–3820.

[21] X.L. Ma, Q.F. Zhang, G.D. Tian, J.S. Yang and Z.X. Zhu, On Tchebycheff Decomposition Approaches for Multi-objective Evolutionary Optimization, IEEE Trans. Evol. Comput., 22(2) (2018) 226–244.

[22] H. Sato, Analysis of inverted PBI and comparison with other scalarizing functions in decomposition based MOEAs, Journal of Heuristics, 21(6) (2015) 819–849.

[23] S. Yang, S. Jiang, and Y. Jiang, Improving the multiobjective evolutionary algorithm based on decomposition with new penalty schemes, Soft Computing, (2016) 1–15.

[24] R. Wang, Q. Zhang, and T. Zhang, Pareto adaptive scalarising functions for decomposition based algorithms, Cham, Switzerland, Part I (2015) 248–62.

[25] H.L. Liu, F. Gu, and Q. Zhang, Decomposition of a multiobjective optimization problem into a number of simple multiobjective subproblems, IEEE Trans. Evol. Comput., 18(3) (2014) 450–455.

[26] S.Y. Jiang, S.X. Yang, Y. Wang, and X.B. Liu, Scalarizing Functions in Decomposition-based Multiobjective Evolutionary Algorithms, IEEE Trans. Evol. Comput., 22(2) (2018) 296–313.

[27] Q. Zhang, W. Liu, and H. Li, The performance of a new version of MOEA/D on cec09 unconstrained mop test instances, in Evolutionary Computation, 2009. CEC '09. IEEE Congress on, (2009) 203–208.

[28] A. Zhou and Q. Zhang, Are all the subproblems equally important? resource allocation in decomposition-based multiobjective evolutionary algorithms, IEEE Trans. Evol. Comput., 20(1) (2016) 52–64.

[29] X. Cai, Y. Li, Z. Fan, and Q. Zhang, An external archive guided multiobjective evolutionary algorithm based on decomposition for combinatorial optimization, IEEE Trans. Evol. Comput., 19(4) (2015) 508–523.

[30] H. Li and Q. Zhang, Multiobjective optimization problems with complicated pareto sets, MOEA/D and NSGA-II, IEEE Trans. Evol. Comput., 13(2) (2009) 284–302.

[31] S. Zapotecas-Martinez, B. Derbel, A. Liefooghe, H. Aguirre, and K. Tanaka, Geometric differential evolution in moea/d: a preliminary study, Cham, Switzerland, Part I (2015) 364–376.

[32] W. Peng and Q. Zhang, A decomposition-based multi-objective particle swarm optimization algorithm for continuous optimization problems, Piscataway, NJ, USA, (2008) 534–537.

[33] N. Al Moubayed, A. Petrovski, and J. McCall, D2MOPSO: MOPSO based on decomposition and dominance with archiving using crowding distance in objective and solution spaces, Evol. Comput., 22(1) (2014) 47–77.

[34] L. Ke, Q. Zhang, and R. Battiti, MOEA/D-ACO: A multiobjective evolutionary algorithm using decomposition and antcolony, IEEE Transactions on Cybernetics, 43(6) (2013) 1845–1859.

[35] K. Sindhya, S. Ruuska, T. Haanpaa, and K. Miettinen, A new hybrid mutation operator for multiobjective optimization with differential evolution, Soft Computing, 15(10) (2011) 2041–55.

[36] S. Jiang and S. Yang, An improved multiobjective optimization evolutionary algorithm based on decomposition for complex pareto fronts, IEEE Transactions on Cybernetics, 46(2) (2016) 421–437.

[37] K. Li, Q. Zhang, S. Kwong, M. Li, and R. Wang, Stable matching based selection in evolutionary multiobjective optimization, IEEE Trans. Evol. Comput., 18(6) (2014) 909–923.

[38] Z. Wang, Q. Zhang, M. Gong, and A. Zhou, A replacement strategy for balancing convergence and diversity in MOEA/D, in 2014 IEEE Congress on Evolutionary Computation (CEC), (2014) 2132–2139.

[39] Z. Wang, Q. Zhang, A. Zhou, M. Gong, L. Jiao, Adaptive Replacement Strategies for MOEA/D, IEEE Trans. Evol. Comput., 46(2) (2016) 474–486.

[40] J.J. Palacios Alonso and B. Derbel, On maintaining diversity in MOEA/D: Application to a biobjective combinatorial FJSP, in Proceedings of the 2015 Annual Conference on Genetic and Evolutionary Computation, ser. GECCO '15. New York, NY, USA: ACM, (2015) 719–726.

[41] K. Li, S. Kwong, Q. Zhang, and K. Deb, Interrelationship-based selection for decomposition multiobjective optimization, IEEE Transactions on Cybernetics, 45(10) (2015) 2076–2088.

[42] M. Wu, K. Li, S. Kwong, Y. Zhou, and Q. Zhang, Matching-Based Selection with Incomplete Lists for Decomposition Multi-Objective Optimization, IEEE Trans. Evol. Comput., 21(4) (2017) 554–568.

[43] L. Wang, Q. Zhang, A. Zhou, M. Gong, L. Jiao, Constrained Subproblems in a Decomposition-Based Multiobjective evolutionary Algorithm, IEEE Trans. Evol. Comput., 20(3) (2016) 475–480.

[44] C. Dai, X. Lei, A New Evolutionary Algorithm Based on Decomposition for Multi-objective Optimization Problems, 2016 12th International Conference on Computational Intelligence and Security (CIS), (2016) 33-38.

[45] R. Wang, Z. B. Zhou, and H. ishibuchi, Localized weighted sum method for many-objective optimization, IEEE Trans. Evol. Comput., 22(1) (2018) 3–18.

[46] S.Y. Jiang, S.X. Yang, A Strength Pareto Evolutionary Algorithm Based on Reference Direction for Multi-objective and Many-objective Optimization, IEEE Trans. Evol. Comput., 21(3) (2017) 329–346.

[47] H. Ishibuchi, Y. Setoguchi, H. Masuda, and Y. Nojima, Performance of Decomposition-Based Many-Objective Algorithms Strongly Depends on Pareto Front Shapes, IEEE Trans. Evol. Comput., 21(2) (2017) 169–190.

[48] Y. Qi, X. Ma, F. Liu, L. Jiao, J. Sun, and J. Wu, MOEA/D with adaptive weight adjustment, Evol. Comput., 22(2) (2014) 231– 264.

[49] F. Gu, H.L. Liu, and K. C. Tan, A multiobjective evolutionary algorithm using dynamic weight design method, International Journal of Innovative Computing, Information and Control, 8(5B) (2012) 3677–3688.

[50] X. Cai, Z. Mei, and Z. Fan, A Decomposition-Based Many-Objective Evolutionary Algorithm With Two Types of Adjustments for Direction Vectors, IEEE Transactions on Cybernetics, to be published (2018) 1–14.

[51] M. Asafuddoula, H. K. Singh, and T. Ray, An Enhanced Decomposition-Based Evolutionary Algorithm With Adaptive Reference Vectors, IEEE Transactions on Cybernetics, to be published (2018) 1–14.

[52] Y. Tian, R. Cheng, X. Zhang, F. Cheng, and Y. Jin, An Indicator Based Multi-Objective Evolutionary Algorithm with Reference Point Adaptation for Better Versatility, IEEE Transactions on Cybernetics, to be published (2017) 1–14.

[53] T. Murata and M. Gen, Cellular genetic algorithm for multi-objective optimization, in Proc. of the Fourth Asian Fuzzy System Symposium, (2002) 538-542.

[54] T. Murata, H. Ishibuchi, and M. Gen, Specification of genetic search directions in cellular multi-objective genetic algorithms, in Evolutionary Multi-Criterion Optimization. Berlin, Germany: Springer, (2001) 82–95.

[55] K. Deb and H. Jain, An evolutionary many-objective optimization algorithm using reference-point based non-dominated sorting approach, part I: solving problems with box constraints, IEEE Trans. Evol. Comput., 18(4) (2014) 577-601.

[56] K. Deb and R. B. Agrawal, Simulated binary crossover for continuous search space, Complex Syst., 9 (1995) 115–148.

[57] R. Xu and D. Wunsch, Survey of clustering algorithms, IEEE Transactions on neural networks, 16(3) (2005) 645–678.

[58] B. Kr. Patra, S. Nandi, P. Viswanath, A distance based clustering method for arbitrary shaped clusters in large datasets, Pattern Recognition, 44 (2011) 2862–2870.

[59] S. Huband, P. Hingston, L. Barone, and L. While, A review of multiobjective test problems and a scalable test problem toolkit, IEEE Trans. Evol. Comput., 10(5) (2006) 477–506.

[60] Q. Zhang et al., Multiobjective optimization test instances for the CEC 2009 special session and competition, Dept. Comput. Sci. Electron. Eng., Univ. Essex, Colchester, U.K., and Dept. Electr. Electron. Eng., Nanyang Technol. Univ., Singapore, Tech. Rep. (2008) CES–487.

[61] E. Zitzler, K. Deb, L. Thiele, Comparison of multiobjective evolutionary algorithms: Empirical results, Evol. Comput., 8(2) (2000) 173-195.

[62] K. Deb, L. Thiele, M. Laumanns, E. Zitzler, Scalable test problems for evolutionary multiobjective optimization, in Evolutionary Multiobjective Optimization (Advanced Information and Knowledge Processing), A. Abraham, L. Jain, R. Goldber, Eds. London, U.K.: Springer, (2005) 105-145.

[63] E. Zitzler, L. Thiele, M. Laumanns, C. Fonseca, and V. da Fonseca, Performance assessment of multiobjective optimizers: An analysis and review, IEEE Trans. Evol. Comput., 7(2) (2003) 117–132.

[64] P. Bosman and D. Thierens, The balance between proximity and diversity in multiobjective evolutionary algorithms, IEEE Trans. Evol. Comput., 7(2) (2003) 174–188.

[65] S. Das, P. N. Suganthan, Differential Evolution: A Survey of the State-of-the-Art, IEEE Trans. Evol. Comput., 15(1) (2011) 4-31.

[66] Y. Yuan, H. Xu, B. Wang, and X. Yao, A new dominance relation based evolutionary algorithm for many-objective optimization, IEEE Trans. Evol. Comput., 20(1) (2016) 16–37.

[67] J. Alcala-Fdez, L. Sanchez, S. Garcia, M.J. del Jesus, S. Ventura, J.M. Garrel, J.Otero, C. Romero, J. Bacardit, V.M. Rivas, J.C. Fernandez, F. Herrera, KEEL: a software tool to assess evolutionary algorithms for data mining problems, Soft Comput., 13 (2009) 307–318.

[68] K. Deb, M. Mohan, S. Mishra, Towards a Quick Computation of Well-Spread Pareto-Optimal Solutions, In: C.M. Fonseca et al. (Eds): EMO, Springer-Verlag Berlin Heidelberg, 2632 (2003) 222-236.

[69] Y. Xiang, Y. R. Zhou, M. Q. Li, A Vector Angle based Evolutionary Algorithm for Unconstrained Many-Objective Optimization, IEEE Trans. Evol. Comput., 21(1) (2017) 131-152.

[70] Y. Tian, X. Zhang, R. Chen, Y. Jin, A Multi-objective Evolutionary Algorithm Based on an Enhanced Inverted Generational Distance Metric, in 2016 IEEE Congress on Evolutionary Computation (CEC), (2016) 5222–5229.

[71] M. Emmerich, N. Beume, B. Naujoks, An EMO Algorithm Using the Hypervolume Measure as Selection Criterion, In: C. A. Coello Coello et al. (Eds): EMO, Springer-Verlag Berlin Heidelberg, 3410 (2005) 62-76.

[72] M. Wu, K. Li, S. Kwong, Q. Zhang, J. Zhang, Learning to Decompose: A paradigm for Decomposition-Based Multiobjective Optimization, IEEE Trans. Evol. Comput., in press, doi: 10.1109/TEVC.2018.2865931, 2018.

[73] Y. Yuan, H. Xu, B. Wang, B. Zhang, and X. Yao, Balancing convergence and diversity in decomposition-based many-objective optimizers, IEEE Trans. Evol. Comput., 20(2) (2016) 180-198.

[74] R. Cheng, M. Li, Y. Tian, X. Zhang, S. Yang, Y. Jin, X. Yao, A benchmark test suite for evolutionary many-objective optimization, Complex and Intelligent Systems, 3(1) (2017) 67-81.